iScience

CellPress
OPEN ACCESS

Article

Behavioral analysis through the lifespan of *disc1* mutant zebrafish identifies defects in sensorimotor transformation

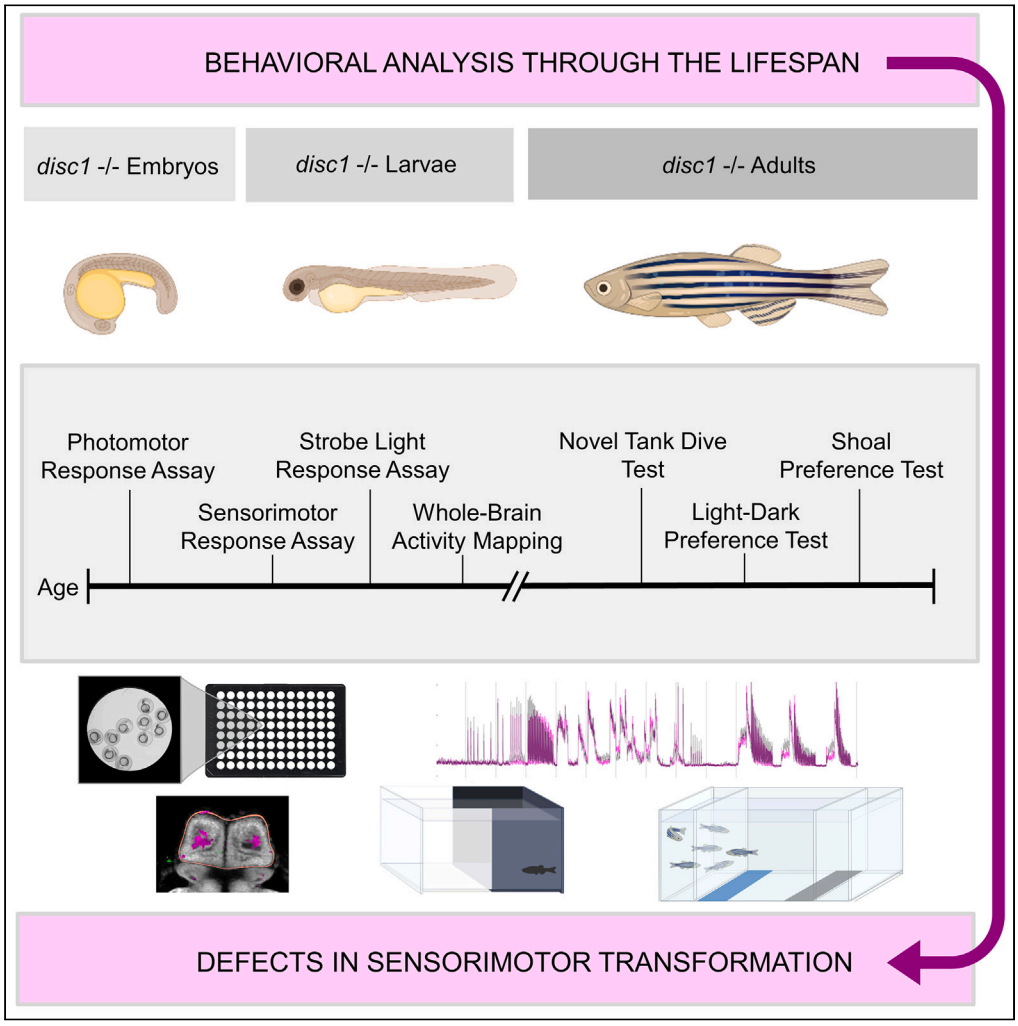

Brock R. Pluimer, Devin L. Harrison, Chanon Boonyavairoje, ..., Randall T. Peterson, Summer B. Thyme, Anjali K. Nath

anath1@bidmc.harvard.edu

Highlights

disc1 mutants display blunted behavioral responses to sensory stimuli

Neural activity in the cerebellum, tectum, and pallium is increased in *disc1* mutants

disc1 mutants exhibit decreased anxiogenic behavior and increased exploration behavior

Loss of *disc1* leads to sex-specific differences in behaviors

Pluimer et al., iScience 26, 107099
July 21, 2023
https://doi.org/10.1016/j.isci.2023.107099

iScience

CellPress
OPEN ACCESS

Article

Behavioral analysis through the lifespan of *disc1* mutant zebrafish identifies defects in sensorimotor transformation

Brock R. Pluimer,[1] Devin L. Harrison,[1] Chanon Boonyavairoje,[2] Eric P. Prinssen,[3] Mark Rogers-Evans,[3] Randall T. Peterson,[4] Summer B. Thyme,[5] and Anjali K. Nath[1,2,6,7,8,*]

SUMMARY

***DISC1* is a genetic risk factor for multiple psychiatric disorders. Compared to the dozens of murine *Disc1* models, there is a paucity of zebrafish *disc1* models—an organism amenable to high-throughput experimentation. We conducted the longitudinal neurobehavioral analysis of *disc1* mutant zebrafish across key stages of life. During early developmental stages, *disc1* mutants exhibited abrogated behavioral responses to sensory stimuli across multiple testing platforms. Moreover, during exposure to an acoustic sensory stimulus, loss of *disc1* resulted in the abnormal activation of neurons in the pallium, cerebellum, and tectum—anatomical sites involved in the integration of sensory perception and motor control. In adulthood, *disc1* mutants exhibited sexually dimorphic reduction in anxiogenic behavior in novel paradigms. Together, these findings implicate *disc1* in sensorimotor processes and the genesis of anxiogenic behaviors, which could be exploited for the development of novel treatments in addition to investigating the biology of sensorimotor transformation in the context of *disc1* deletion.**

INTRODUCTION

Disrupted-In-Schizophrenia 1 (*DISC1*) was originally identified to co-segregate with schizophrenia, bipolar disorder, and major depression, and growing evidence now demonstrates that human *DISC1* variants also confer risk to endophenotypes that underlie multiple neurodevelopmental disorders, including autism spectrum disorder, attention-deficit/hyperactivity disorder, and Asperger's syndrome.[1–9] The diversity of endophenotypes associated with *DISC1* mutations in patients is mirrored by the diversity of phenotypes observed in murine *Disc1* genetic models. Currently, there are over a dozen genetic models to study *Disc1*-dependent phenotypes.[10–13] Moreover, many of the murine *Disc1* genetic models exhibit opposing or unique behavioral phenotypes.[10,12,13] These differences suggest possible environmental influences on behavior in the context of *Disc1* deletion. Further complicating the analysis of the growing number of murine lines, there could be age-dependent functions of this gene, and it is challenging to characterize behavior with a battery of assays throughout the lifespan.[10–13]

Zebrafish is an ideal model organism to overcome these challenges and decipher gene-environment interactions in behavioral neuroscience.[14,15] Each week, a mating pair can produce ≥200 fertilized eggs. Due to their fecundity, rapid *ex utero* development, and modest laboratory footprint, these small vertebrate organisms are uniquely positioned for large-scale behavioral phenotyping and high-throughput chemical screening. Multiple paradigms and experimental permutations can be tested in a short period of time. Moreover, by 5 days post-fertilization (dpf), larval zebrafish possess all major sensory organs and neurotransmitter systems in addition to displaying a rich repertoire of complex neurobehaviors including hunting, avoidance of predators, group interactions, learning and memory, and prepulse inhibition.[15–22] Zebrafish provide a unique opportunity to assess behaviors from as early as 1 dpf (embryonic stage) to 7 dpf (an equivalent developmental stage to post-natal mammals),[21,23–25] in addition to testing classical adult paradigms of behavior.[26–29] Thus, zebrafish is a tractable model for behavioral phenotyping through the lifespan.

Prior studies in zebrafish have investigated the functions of *disc1* in early neurodevelopmental processes.[30–36] These studies demonstrate that *disc1* plays a conserved role in neural development. Moreover, the biological and molecular functions of Disc1 are conserved between humans and zebrafish. For

[1]Cardiovascular Research Center, Massachusetts General Hospital, Charlestown, MA 02129, USA

[2]Division of Cardiovascular Medicine, Beth Israel Deaconess Medical Center, Boston, MA 02215, USA

[3]Roche Pharmaceutical Research and Early Development, Roche Innovation Center Basel, Grenzacherstrasse 124, 4070 Basel, Switzerland

[4]Deparment of Pharmacology and Toxicology, College of Pharmacy, University of Utah, Salt Lake City, UT 84112, USA

[5]Department of Neurobiology, University of Alabama, Birmingham, AL 35294, USA

[6]Broad Institute, Cambridge, MA 02142, USA

[7]Department of Medicine, Harvard Medical School, Boston, MA 02115, USA

[8]Lead contact

*Correspondence: anath1@bidmc.harvard.edu

https://doi.org/10.1016/j.isci.2023.107099

example, abnormal axonogenesis and defects in Wnt-mediated neural development caused by loss of *disc1* in zebrafish were rescued by the co-injection of human *DISC1* mRNA.[30,33] While the majority of prior studies on *disc1* in zebrafish were focused on understanding its role in neurodevelopment,[30–36] investigations into the behavioral effects of *disc1* mutations in zebrafish have only just begun.[34] Consequently, the development of *disc1*-mediated behavioral models in zebrafish has been lagging that of murine models. Dependent on the specific *Disc1* mutant line being tested, *Disc1* mutations in mice affect anxiety, sociability, and depressive-like behaviors.[10–13,37–43] In both mice and humans, carriers of DISC1 mutations exhibit defects in sensorimotor behaviors such as acoustic startle and sensory gating.[10,38] Finally, sex differences in behavioral responses were reported in *disc1* murine models.[44–46] In the present study, our aims were 1) to decipher gene-environment interactions of *disc1* through lifespan in zebrafish, and 2) to identify behavioral endpoints in *disc1* mutants that could be leveraged for future high-throughput chemical screens.

Here, we generated zebrafish *disc1* mutants and subjected them to neurobehavioral testing across multiple paradigms throughout their lifespan. In embryos, larvae, and adults, we measured responses to visual and auditory stimuli, and tested paradigms of fear, anxiety, and socialization. As early as 28 h postfertilization (hpf), *disc1* mutants were behaviorally distinct from wild-type animals and exhibited abrogated sensorimotor behaviors. Differences in responses to sensorimotor stimuli in *disc1* mutant embryos and larvae were present in multiple testing paradigms and preceded sex-dependent differences in anxiety in adulthood. Finally, we conducted whole-brain optical imaging to map neuronal activity in *disc1* mutant brains and compared it to existing data on schizophrenia-associated genes collected by our group. In summary, this new mutant line provides a tractable neurogenetic model to study sensorimotor pathways and the genesis of anxiogenic behaviors in the context of genetic loss of *disc1*. In addition, we identified behavioral endpoints that will enable the chemical screening of small molecules in *disc1* mutants; by leveraging the exact same behavioral phenotyping platforms that are used for high-content screening, we set the stage for large-scale chemical screens aimed at discovering novel pharmaceuticals to reverse the sensorimotor defects in carriers of *disc1* mutations.

RESULTS

Generation of *disc1* mutant zebrafish

We used CRISPR-Cas9 genome editing to target exon 2 (Figures 1A and 1B), as it is present in all annotated zebrafish Disc1 isoforms. The Cas9 target site was upstream of the putative protein-protein binding domains (Figure 1C).[30,47] One mutant exhibited a 20-nucleotide deletion starting at base pair +129 (Figure 1B), which is expected to cause a frameshift, the generation of a premature translational stop codon, and the formation of a predicted truncated protein consisting of 16-amino acids (Figure 1C, red line denotes predicted truncated mutant protein). The founder was raised to adulthood and outcrossed to wild-type (WT) zebrafish. Genotyping and confirmation of knockout were performed by PCR fragment length analysis (Figure S1) and by Western blot using an antibody directed to an internal sequence (aa 511-527) (Figure 1D). WTs displayed an expected band at ~100 kD while *disc1* homozygous mutants lacked this band, confirming that the truncated allele results in the loss of Disc1 protein. The expected Mendelian ratio was observed in 3-month-old adults derived from heterozygous crosses (Figure 1E, n = 451). Further, the mutant larvae exhibited normal gross morphology at 6 dpf (Figure 1F), and adults were fertile and lived a normal lifespan. Next, we sought to characterize the behavioral responses of *disc1* homozygous mutant embryos, larvae, and adults using a battery of behavioral assays (Figure 1G).

The photomotor response is absent in *disc1* mutant embryos

Prior to the development of a functional visual system, exposure to high intensity white light induces rapid, rhythmic tail coiling movements in zebrafish embryos. This nonvisual light-driven motor behavior, termed the photomotor response, occurs between 24 and 30 h postfertilization (hpf) and is controlled by photosensitive neurons in the hindbrain.[48] The photomotor response assay was designed to capture the robust and reproducible series of motor behaviors induced by photo-stimulation, and consists of four discrete phases: pre-stimulus background phase, latency phase, excitation phase, and refractory phase.[23] In dark-adapted embryos that were previously loaded into 96-well plates, basal motion is acquired for 9 s (pre-stimulus background phase). Next, an intense visual wavelength light stimulus is delivered for 1 s resulting in a brief latency phase (1 s) followed by vigorous tail coiling that lasts for 5 s (excitation phase). Subsequently, a second light pulse does not elicit vigorous movement (refractory phase) (Figures 2A and 2B). These stereotypic movements are registered as motion indexes (MI) that are calculated by frame differencing serial images from digital videos (Figure 2B).[23]

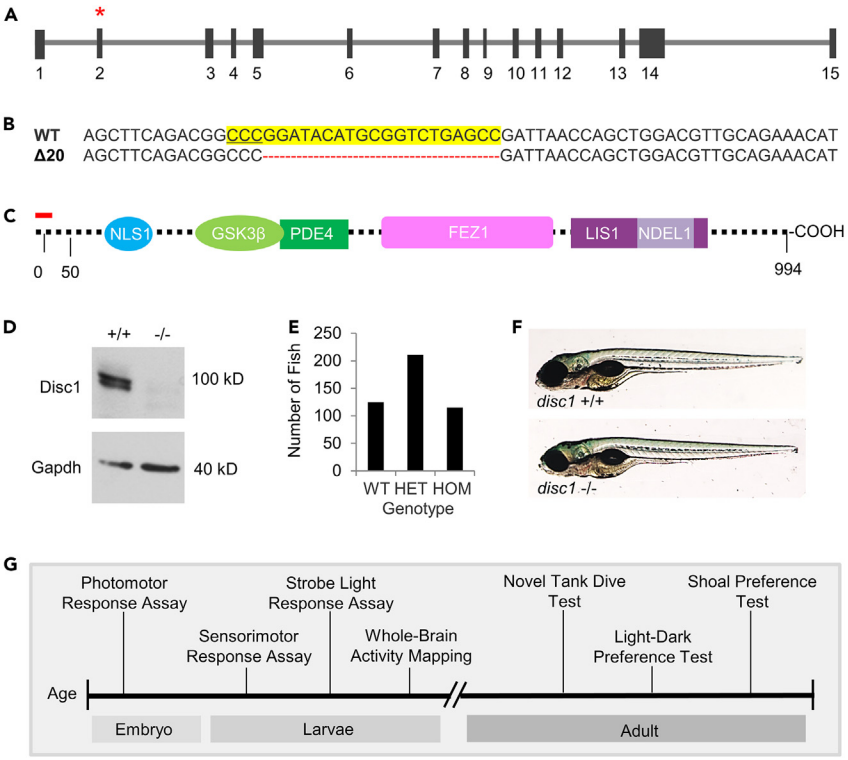

Figure 1. Generation of the *disc1* mutant genetic model in zebrafish

(A) Representation of the 15 exon *disc1* gene. Red asterisk indicates the site targeted.

(B) The CRISPR-Cas9 target site is highlighted in yellow, with the PAM underlined. A mutant line with a 20-base pair deletion (denoted by red dashes) was identified.

(C) Depiction of the putative Disc1 protein domains. The red line indicates the predicted length of the truncated protein in *disc1* mutants.

(D) Western blot of Disc1 protein in lysates from *disc1* WT and HOM larvae at 7 dpf (25 larvae per lane).

(E) Ratio of genotypes in offspring generated by *disc1* heterozygous incrosses (n = 451; age = 3 months).

(F) Light micrographs of *disc1* WT and HOM larvae at 7 dpf.

(G) Diagram depicting the timeline of neurobehavioral assays conducted through lifespan.

As expected, during the excitation phase, 28 hpf WT embryos exhibited a significant increase in motion index as compared to their baseline motion (Figure 2C; MI = 149.2 $\pm$ 13.0 versus 64.5 $\pm$ 5.9; p = 0.001; FDR $q < 0.0001$), followed by a refractory period in which they did not respond to a second pulse of light (MI = 39.9 $\pm$ 3.2). In contrast to this normal response to photo-stimulation, *disc1* mutants did not exhibit a significant increase in motion after the first light pulse as compared to their baseline motion (Figure 2C). Moreover, the maximal motion index reached during the excitation phase was ~26% lower in *disc1* mutants as compared to that of WTs in the excitation phase (p = 0.01; FDR $q = 0.002$). These data indicate that light-induced excitation is not present in *disc1* homozygous embryos. These findings were not due to developmental delay as embryonic staging by developmental landmarks and by somite number was normal (Figures S2A and S2B). In addition, morphological defects in muscle structure were not detected (Figures S2C-S2J).

Following the excitation phase, WT animals did not respond to a second light pulse delivered at t = 20 s (Figure 2C; refractory phase). Similar to WTs, *disc1* mutants did not respond to the second light stimulus. Interestingly, the motion index in the refractory phase decreased to ~40% below the pre-stimulus baseline level in mutants (p = 0.001; FDR $q < 0.0001$) similar to the ~41% decrease observed in WTs (p = 0.0005; FDR $q < 0.0001$) (Figure 2C). The finding that mutants exposed to a second light pulse decreased their MI may indicate that *disc1* mutants perceive the first light stimuli but did not respond by increasing motor activity. Cumulatively, these data demonstrate that genetic loss of *disc1* affects behavioral responses, specifically the nonvisual light-driven motor circuit located in the zebrafish hindbrain, as early as 28 hpf.

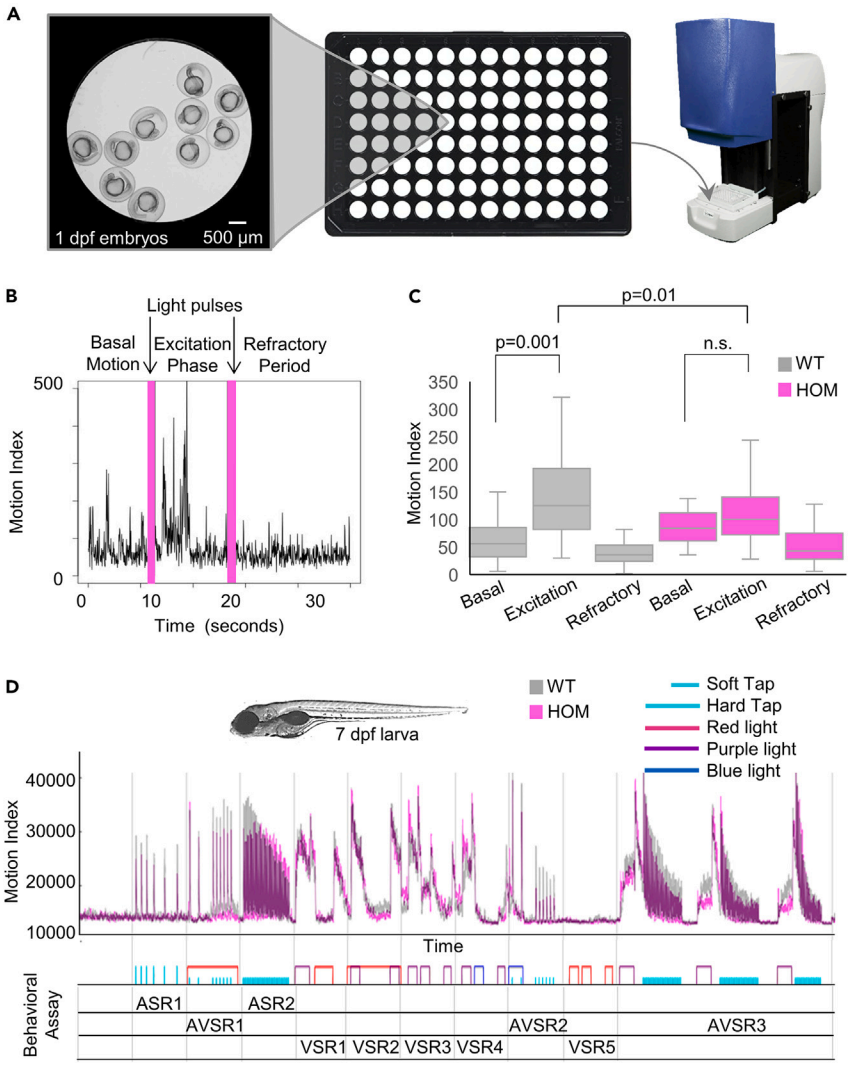

Figure 2. *disc1* mutant embryos and larvae display blunted behavioral responses to sensory stimuli

(A) Overview of the photomotor response assay: Ten embryos (28 hpf) per well were loaded into 96-well plates and motion was measured using the ZebraBox.

(B) Example motion index graph. For each well, basal motion was captured, followed by an excitation period induced by a light stimulus (denoted by a magenta vertical bar), and a refractory period in which a second light stimulus (denoted by a magenta vertical bar) did not elicit motion.

(C) Box and whisker plot showing motion indexes for the basal, excitation, and refractory phases in WT (gray) and mutant (magenta) embryos (n = 48 wells per genotype). The box in the plot represents the 25th percentile to the 75th percentile, the line across the box represents the median, and the whiskers are the maximum and minimum data-point values.

(D) Behavioral profile generated in 7 dpf larvae using a battery of sensory and acoustic stimuli demonstrating decreased motor output in *disc1* mutants in response to auditory stimuli. Plot shows the average motion index of WT (gray) and *disc1* mutant (magenta) larvae (8 larvae per well, 36 wells per genotype). The x-and y axes indicate time and the motion index, respectively. Behavioral assay names and their order in the run are indicated below the x axis. AS = auditory stimulus, VS. = visual stimulus and AV = auditory plus visual stimulus.

disc1 mutant larvae exhibit blunted behavioral responses to auditory stimuli

We next sought to determine the behavioral responses elicited by a range of sensory stimuli in *disc1* mutants. To measure sensorimotor behavioral responses, we used a platform that we previously developed in which 7 dpf larvae are loaded into 96-well plates and then placed into an enclosed behavioral apparatus to capture motion index for 10 serial behavioral assays.[25] The 10 assays use combinations of visual and auditory stimuli: two acoustic stimulus response assays (ASR1 and ASR2), five visual stimulus response assays

(VSR1-VSR5), and three combined acoustic and visual stimulus response assays (AVSR1-AVSR3). Previously, using this platform, we demonstrated that visual, auditory, and combined stimuli induce unique and robust behavioral profiles.[25]

After an acclimation period to the enclosed platform (in the dark), the basal motion was measured. *disc1* WT and mutant larvae displayed similar baseline motion prior to the start of stimulus delivery (WT MI = 13601 $\pm$ 972 versus HOM MI = 14363 $\pm$ 2190; p = n.s.). Visual stimuli (red, blue, and purple light) elicited a similar motion index in *disc1* mutants as compared to wild-type animals (VSR1-5; Figure 2D). For example, as shown in VSR1, violet light (405 nm) rapidly increased motor activity and when the light was turned off, the animals immediately stopped moving; by contrast, red light did not affect motor activity (Figure 2D). When red (600 nm) was paired with violet light, the sharp decrease in motion was lost. Instead, the activity slowly decayed in the presence of red light (VSR2).

In acoustic stimulus assays, *disc1* mutants exhibited a reduction in motion indexes. In response to a series of one soft tap per second for 30 s (ASR2; Figure 2D), WTs initially responded with a high motion index, which slowly tapered over the 30-s assay as they habituated. In contrast, *disc1* mutants never reached the peak of motion as compared to WTs (HOM MI = 28726 $\pm$ 4523 versus WT MI = 37108 $\pm$ 5879; p = 0.003). In addition, the motion index in mutants remained steady for ~15 s, and then tapered off while in WTs the peak response occurred almost immediately and then tapered off. In combinational acoustic and visual assays (AVSR1-3), *disc1* mutants also responded with less motion. Together, these data demonstrate a defect in motor output following repeated auditory stimulation in *disc1* mutants.

Brain-wide mapping of neural activity in *disc1* mutants following auditory stimulus

In contrast to classical single-neuron mapping in mammals, the optical clarity of zebrafish allows for comprehensive whole-brain mapping. Neuronal activity can be measured in zebrafish brains using phosphorylated extracellular-signaling-regulated kinase (phospho-ERK), a marker of active neurons, followed by confocal microscopy. A whole-brain activity map is then generated using a nonlinear volume registration algorithm.[49] Multiple brains are registered into the Z-brain atlas and statistical differences between the groups (mutant and sibling controls) are calculated.[49] Leveraging this technique, we interrogated gene-function relationships of *disc1* in the zebrafish brain.

As *disc1* mutant larvae displayed differences in sensorimotor behaviors that included auditory stimuli (Figure 2D and Table 1), we chose to define activity maps in the presence of an auditory stimulus. Following an acclimation period in our behavioral platform, a single high magnitude acoustic stimulus (70 dB) was delivered and 2 min later the 7 dpf larvae were fixed. A 2-min delay elicits the highest levels of phospho-ERK.[49] Sibling control fish were exposed to the exact same conditions, as the groups were mixed and genotyped following imaging. We detected increased activity throughout the entire brain in *disc1* mutants compared to controls (Figures 3A and 3B). The most prominent bilateral activity was in the pallium and cerebellum in addition to the tectum (Figures 3C-3E and S3A-S3D; n = 38-44 per genotype), and these activity patterns were replicated in a second experiment (Figure S4). In addition, there were no differences at baseline, in unstimulated animals. Importantly, deformation-based morphometry[50] using the total-ERK stain revealed no apparent structural differences in the mutant brains (Figure S5). Thus, these results indicate that the abnormal sensorimotor behavioral responses in *disc1* mutants are likely due to differences in neural circuit function and not to major changes to brain development or morphology.

We next compared the *disc1* mutant activity patterns to those produced for a large set of zebrafish mutants for schizophrenia-associated genes[51]; *disc1* mutant neural activity maps were not previously published in this dataset. We found that of the 132 mutants *cacna1c* heterozygous loss-of-function was the most similar. In contrast to the increased activity in *disc1* mutant brains, the *cacna1c* mutants showed decreased activity in similar areas (Figures 3F-3K). While the direction of these activity changes differs, the similar pattern indicates a disruption in overlapping circuitry in these two models.

Innate fear response is abrogated in *disc1* mutant larvae

We next sought to determine the effect of fear and anxiety paradigms in our *disc1* mutants. We evaluated the behavioral response to a stimulus that invokes the innate fear response in 7 dpf larvae. Similar to most other animals, zebrafish respond to aversive stimuli by exhibiting defensive behaviors such as freezing and escaping. In zebrafish, encountering aversive stimuli such as bright light, moving shadows, or predators,

Table 1. Summary of Behavioral Responses in *disc1* Mutants

Behavioral Assay	Age	Phenotype	Effect in *disc1* Mutants	Sex-Effect
Photomotor response assay	28 hpf	Light-induced excitation	absent	N/A
		Refractory period	present	N/A
		Photomotor response	absent	N/A
Sensorimotor response assay	7 dpf	Visual stimuli (red, purple or blue light)	–	N/A
		Acoustic stimuli (soft taps or hard taps)	↓	N/A
		Combination of visual and acoustic stimuli	↓	N/A
		Sensorimotor responses	↓	N/A
Strobe light response assay	7 dpf	Innate fear response	↓	N/A
Novel tank diving test	adult	Total time and average time per visit in the top zone	↑	Male
		Distance traveled in the top zone	↑	Male
		Latency to first entry into the top zone	↓	Female
		Number of transitions	–	No
		Mean speed	↓	No
		Anxiogenic behavior	↓	Male
Light-dark preference test	adult	Latency to first entry into the light zone	↓	No
		Total time in light zone	↑	No
		Average time per visit in the light zone	↑	Male
		Number of transitions	–	No
		Scototaxis	absent	No
Shoal preference test	adult	Total visit time and average time per visit social zone	–	No
		Total visit time and average time per visit asocial zone	–	No
		Shoal preference	–	No
Shoal cohesion	adult	Average pairwise fish-fish distance	↓	N/A
		Average distance to furthest neighbor	↓	N/A
		Shoal cohesion	↑	N/A

hpf: hours postfertilization; dpf: days post-fertilization; ↓ indicates decreased response; ↑ indicates increased response; – indicates normal response; N/A indicates sex not known.

evokes active or passive threat response (escaping or freezing behavior, respectively).[52,53] This innate fear response can be modeled using the strobe light response (SLR) assay.[24] In this assay, 7 dpf animals (n = 10) are loaded into 96-well plates and placed in a dark chamber with an infrared camera that records locomotor activity in each well. Alternating 1-min intervals of darkness and 10 Hz strobe light invokes threat response behavior, which is quantified by measuring the overall motion in each well (motion index).

During the dark intervals, WT zebrafish actively and freely swam in their wells (Figure 4A; solid black bars). In contrast, the strobe light induced rapid onset hypo-locomotion and freezing behavior as demonstrated by the motion index at t = 60-120 s (Figure 4A; broken black bars) as compared to the motion index at t = 0-60 s in the dark-interval period. Subsequently, when the next dark interval began at t = 120 s the animals immediately returned to actively swimming in their wells. Thus, the innate fear response was present in 7 dpf WT zebrafish as demonstrated by the substantially decreased average motion indexes during strobe light intervals (Figure 4A, the average motion is indicated by the red line) as compared to dark intervals (Figure 4A, the average motion is indicated by the blue line). *disc1* mutants also responded to strobe light by freezing (Figure 4B), however, there was a difference in latency of the response in *disc1* mutants as compared to wildtypes.

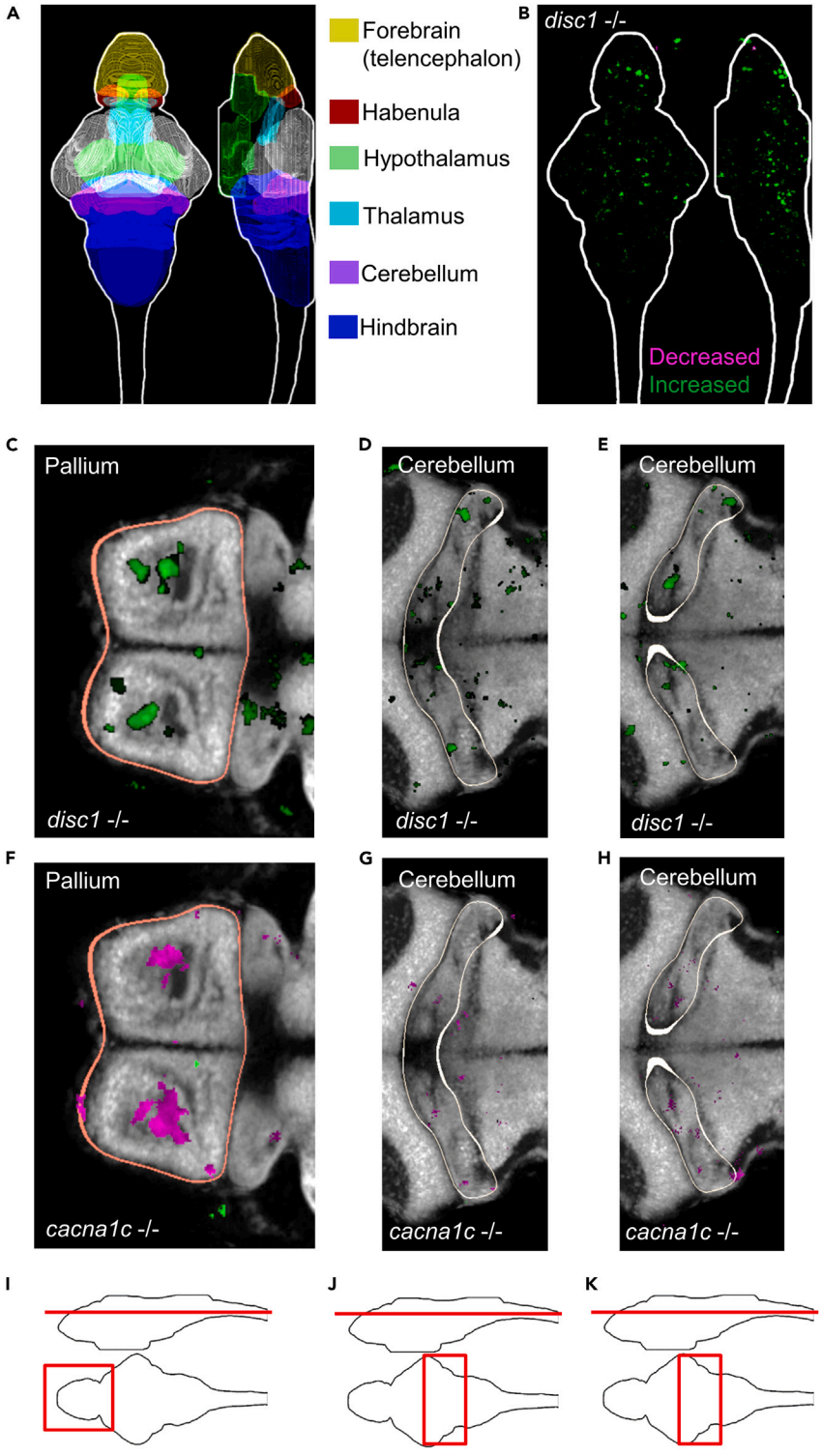

Figure 3. Brain-wide mapping of neural activity in *disc1* mutants following acoustic stimulus

(A) Color coded diagram highlighting several structures in the larval zebrafish brain at 7 dpf.

(B) Sum-of-slices projections (x- and z-axes) of significant differences between *disc1* mutant and sibling control groups (n = 44 HOM and n = 38 sibling controls). Increased versus decreased neuronal activity in *disc1* mutants is displayed as green and magenta, respectively.

Figure 3. *Continued*

(C-H) Image slices showing the specific brain subregions with significant differences in neuronal activity in (C-E) *disc1* and (F-H) *cacna1c* mutants. Images of activity in the (C,F) pallium (outlined in orange) and (D-E), (G-H) cerebellum (outlined in white) demonstrating increased activity differences in these regions in *disc1* mutants and decreased activity differences in these regions in *cacna1c* mutants.

(I-K) Diagrams indicating the spatial location of the image slices displayed in panels C/F, D/G, and E/H, respectively.

Upon closer inspection of the behavioral profiles, WTs and *disc1* mutants exhibited uniform and similar levels of activity in the dark (Figures 4C-4E). By contrast, during the strobe light, hypo-locomotion was abrogated in *disc1* mutants (Figures 4F-4H); at t = 71, the motion index of *disc1* mutants was 31% higher than that of WTs (Figure 4H; 0.81 $\pm$ 0.20 versus 0.60 $\pm$ 10.13; p = 0.0004). Over the next 20 s (t = 71-90), the motion index for mutants was approximately twice that of WTs (t = 75: 0.86 $\pm$ 0.16 versus 0.48 $\pm$ 0.12, p = 0.0001; t = 80: 0.82 $\pm$ 0.16 versus 0.34 $\pm$ 0.08, p = 0.004; t = 85: 0.59 $\pm$ 0.13 versus 0.22 $\pm$ 0.06, p = 0.010). During the last 30 s, both WTs and mutants froze for the remaining 30 s of the strobe light. Together, these results indicate that the innate fear response to a threatening stimulus is present but partially suppressed in *disc1* mutant larvae.

disc1 mutants exhibit decreased anxiogenic behavior and increased exploration behavior in a novel environment

We next sought to assess the behavior of adult mutants in paradigms that induce anxiety. To assess anxiety, we used the novel tank diving test—a well-established assay that is the aquatic equivalent to the murine open field test.[26,54] When removed from their home tank and placed into a new tank, zebrafish instinctively dive to the bottom of the tank to seek protection and subsequently spend the majority of the time swimming near the bottom of the tank (Figure 5A). As the animal habituates to the novel environment, it begins to explore. This is evidenced by swimming upwards and engaging in swimming at the top of the tank. Increased time spent in the top zone of the tank indicates low anxiety and increased willingness to explore a new environment, while increased time spent in the bottom zone of the tank indicates high anxiety and decreased willingness to explore a new environment.[26,54]

Adult male zebrafish were gently placed into a novel tank and digital videos of movement were captured using a side-mounted camera. To globally visualize position preference in the novel tank, heat maps were generated based on the time spent in each x-y coordinate of the tank during the 15-min test. As expected, sibling WT fish spent the majority of the time swimming in the bottom zone of the tank (Figure 5B). In contrast to this normal pattern of position preference in the novel tank diving test, the heatmap of *disc1* mutants depicted increased entries into and increased time spent in the top zone of the tank (Figure 5B). Using motion tracking software, we next quantified several parameters of anxiogenic and exploratory behaviors including time spent in each zone, number of visits to the top zone, and average visit time to the top zone. The total time spent in the top zone was significantly greater in *disc1* mutants versus WT siblings (115 $\pm$ 69 versus 57 $\pm$ 63 s, p = 0.01; Figure 5C). In accordance with this result, the total distance traveled in the top zone was significantly approximately twice as much in mutants versus WTs (484 $\pm$ 230 versus 216 $\pm$ 151 cm, p = 0.0004; Figure 5D). Concomitantly, the total distance traveled the bottom zone was significantly less in *disc1* mutants versus WTs (p = 0.01; Figure 5E). Mutants did not exhibit a significant difference in latency time to first entry into the top zone or in the total number of visits to the top zone as compared to WTs (Figures 5F and 5G). However, the average time spent per visit to the top zone was approximately twice as long in *disc1* mutants versus WTs (2.99 $\pm$ 1.83 versus 1.73 $\pm$ 0.56 s, p = 0.009; Figure 5H) leading to increased total time in the top zone. The mean speed of mutants was slower than that of WTs (p = 0.009; Figure 5I), and the total distance traveled in the whole tank was less (p = 0.03; Figure 5J). Cumulatively, these findings indicate that male *disc1* mutants exhibit increased exploratory behavior when placed in a new environment and demonstrate behaviors associated with low anxiety in response to the stress of a novel environment.

disc1 mutants exhibit sex-specific differences in anxiogenic and exploration behaviors

To determine if there are sex-specific differences in our *disc1* mutant line, we next examined the behavior of adult female zebrafish. Female *disc1* mutants did not exhibit significant differences in position preference in the novel tank diving test as reflected by heat maps of the time spent in each x-y coordinate of the tank (Figures 6A and 6B). Moreover, female *disc1* mutant zebrafish did not display significant differences in most of the parameters of anxiogenic behaviors measured as compared to female WT siblings (Figures 6C-6J).

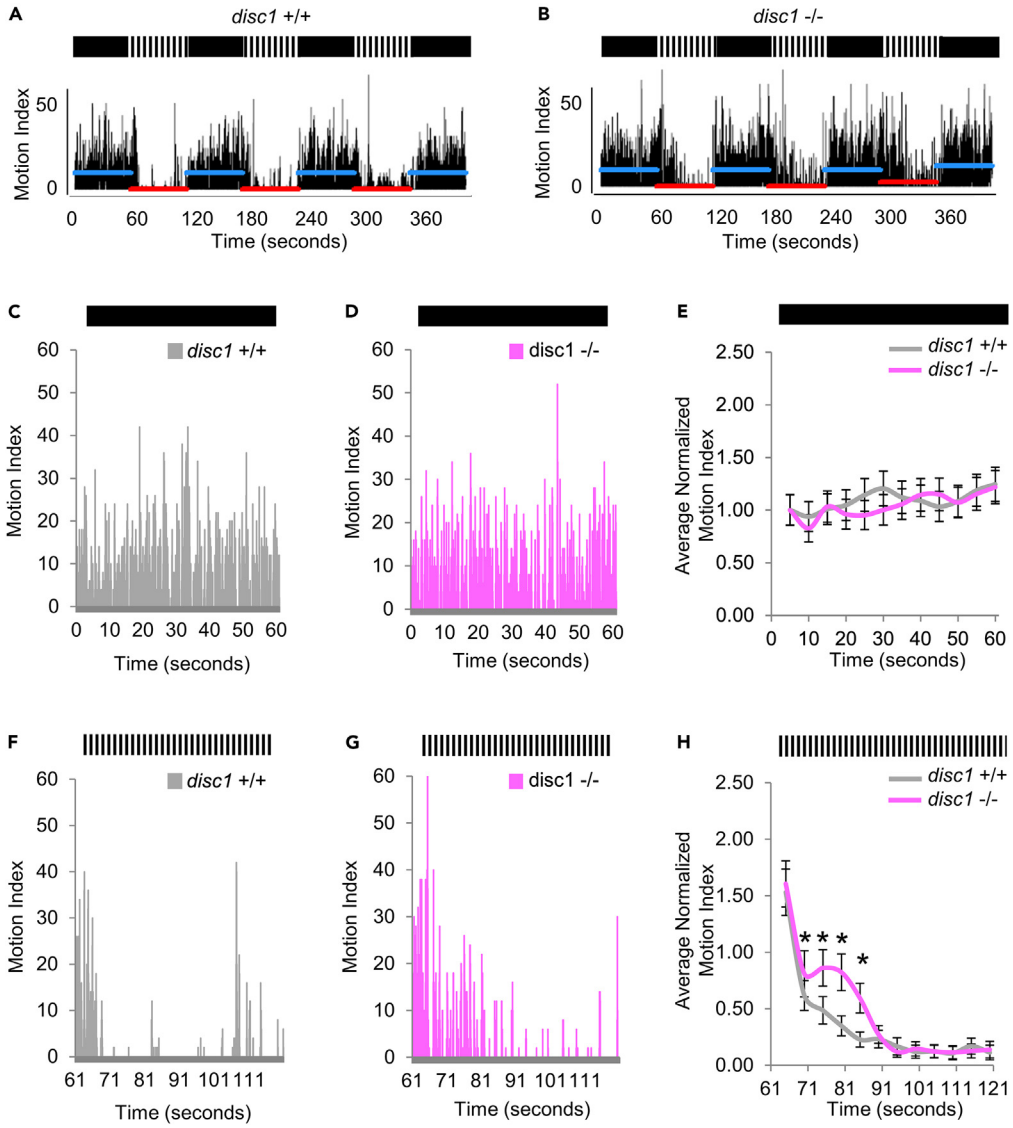

Figure 4. Innate fear response is abrogated in *disc1* mutant larvae

(A and B) Plots of motion index for (A) WT and (B) mutant larvae (7 dpf) in the strobe light response assay. Dark versus strobe light intervals are indicated by the solid black versus the black-and-white panels above the plots.

(C and D) The blue and red lines indicate the average motion index during the dark and strobing light periods, respectively. Representative plots of 60 s of motion during the dark period for (C) WT and (D) mutant larvae.

(E) Graph of average motion index over time (motion binned in 5 s intervals) in WT (gray) and mutant (magenta) larvae demonstrating that both move at a similarly constant level throughout the 60-s dark period (10 larvae per well, 48 wells per genotype).

(F and G) Data is normalized to the WT MI at t = 0. Representative plots of motion during the strobe light period for (F) WT and (G) mutant larvae.

(H) Graph of average motion index over time in WT (gray) and mutant (magenta) larvae demonstrating that, during the strobe light phase and during a specific period (t = 71-90), *disc1* mutants exhibit a higher motion index as compared with WT larvae. Data is normalized to the WT MI at t = 0. * = $p < 0.01$.

Error bars = standard deviation.

The only behavior that was significantly different in female mutants as compared to female WTs was a reduction in latency to first entry into the top zone (96 $\pm$ 69 versus 200 $\pm$ 142 s, $p = 0.007$; Figure 6F); this phenotype was not observed in male mutants. The mean speed of female mutants was slower than female WTs ($p = 0.05$; Figure 6I), a phenotype also observed in males; however, the total distance traveled in

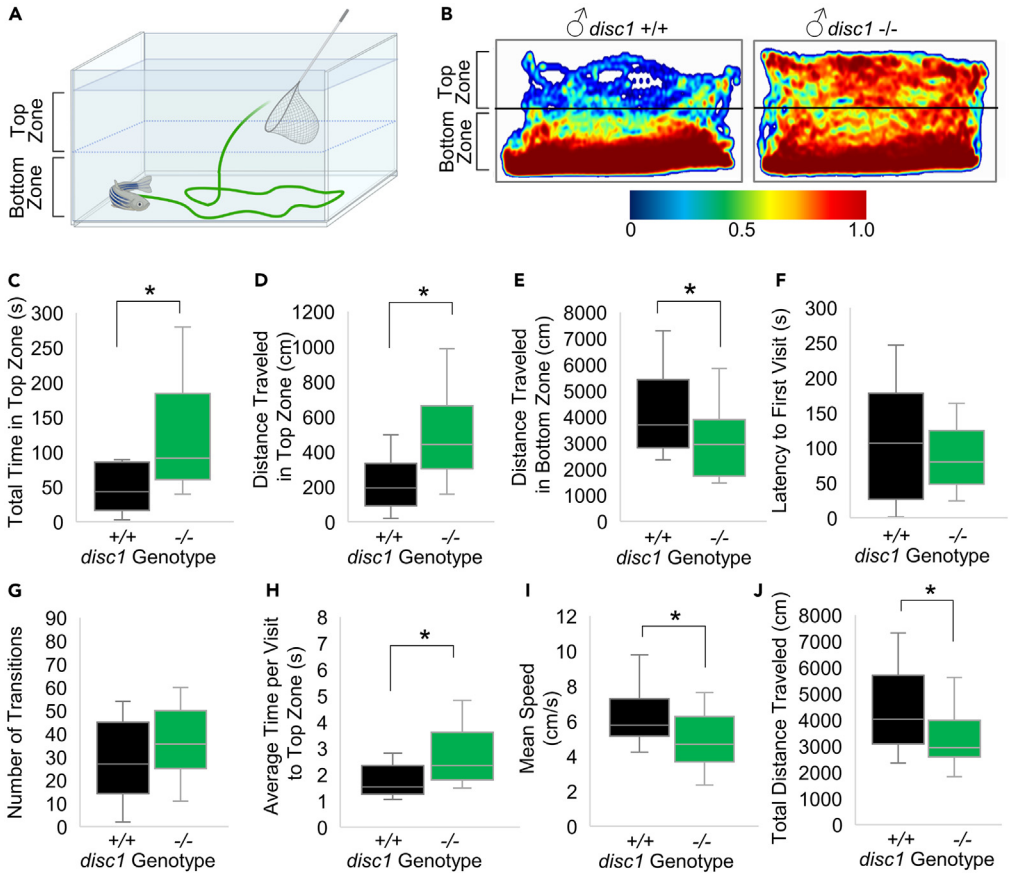

Figure 5. Adult male *disc1* mutants exhibit decreased anxiogenic behavior and increased exploration behavior in a novel environment

(A) Diagram of behavioral testing arena.

(B) Spatiotemporal data (heat maps) depicting the amount of time spent at each location in the testing arena by a representative male WT sibling and male *disc1* mutant (red indicates increased time and blue indicates decreased time).

(C-J) Box and whisker plots of the (C) total time spent in the top zone, (D) distance traveled in the top zone, (E) distance traveled in the bottom zone, (F) latency time to first visit to the top zone, (G) the number of transitions between the top and bottom zone, (H) average time per visit in the top zone, (I) mean speed throughout the duration of the assay, and (J) total distance traveled in the top and bottom zone combined. WTs (black, n = 16 males), HOMs (green, n = 16 males). * = $p < 0.01$. The box in the plot represents the 25th percentile to the 75th percentile, the line across the box represents the median, and the whiskers are the maximum and minimum data-point values. * = $p<0.05$.

the whole tank was not different in females. In summary, these findings indicate that loss of *disc1* leads to differences in several metrics of anxiety and exploratory behaviors in males but not females.

disc1 mutants do not exhibit scototaxis in the light-dark preference test

We next assessed behavior in a conflict-based novelty test. Zebrafish exhibit an innate aversion to brightly illuminated spaces and a marked preference for dark spaces, a behavior termed scototaxis, which can be measured using the light-dark preference test.[27,54] In this assay, a zebrafish is placed in a tank that is half-lit and half-dark (Figure 7A). When placed in this environment, zebrafish have a marked preference for the dark compartment as evidenced by spending more time in that zone. Increased time spent in the light compartment indicates increased risk-taking behavior and a reduction in anxiety-like behavior.[27,54]

disc1 mutants spent more time in the light zone as compared to wildtypes. Male mutants spent 39% more time in the light zone (46 s, $p = 0.02$, FDR $q = 0.009$) as compared to male WTs (Figure 7B) and female mutants spent 29% more time in the light zone (41 s, $p = 0.04$, FDR $q = 0.011$) as compared to female WTs (Figure 7C). *disc1* mutants (males and females) exhibited a shorter latency time to first entry into

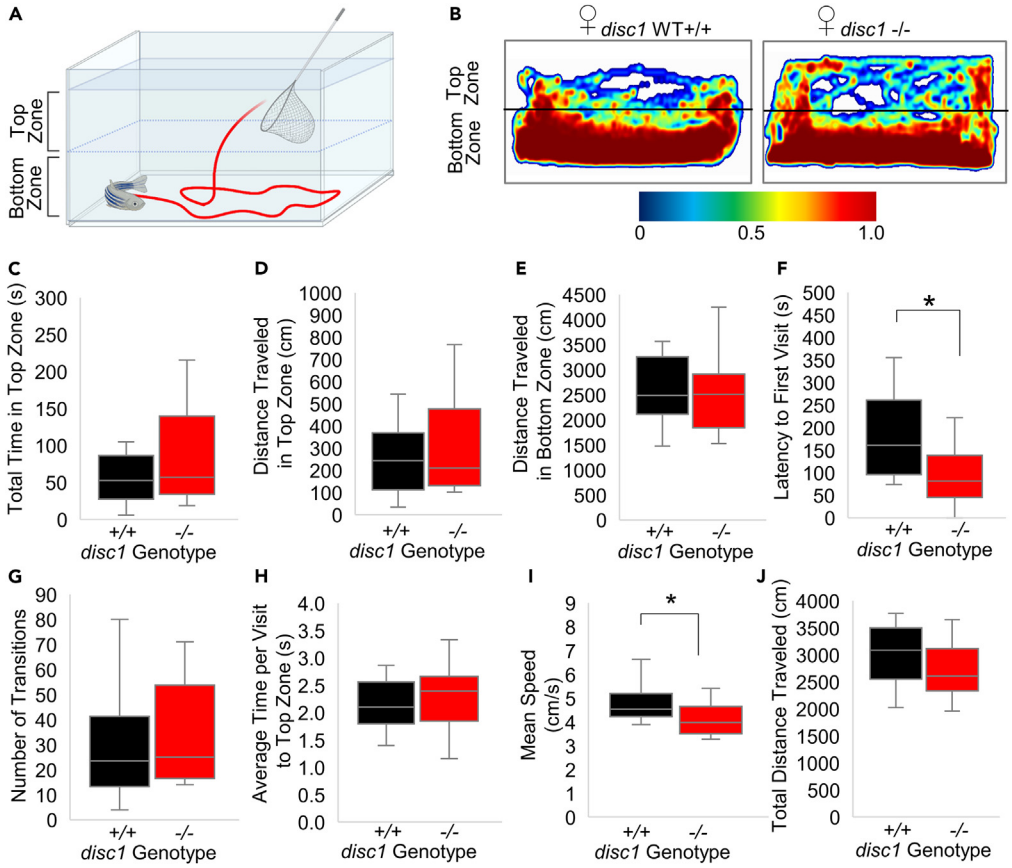

Figure 6. Adult female *disc1* mutants do not exhibit decreased anxiogenic behavior and increased exploration behavior in a novel environment

(A) Diagram of behavioral testing arena.

(B) Spatiotemporal data (heat maps) depicting the amount of time spent at each location in the testing arena by a representative female WT sibling and female *disc1* mutant (red indicates increased time and blue indicates decreased time).

(C-J) Box and whisker plots of the (C) total time spent in the top zone, (D) distance traveled in the top zone, (E) distance traveled in the bottom zone, (F) latency time to first visit to the top zone, (G) the number of transitions between the top and bottom zone, (H) average time per visit in the top zone, (I) mean speed throughout the duration of the assay, and (J) total distance traveled in the top and bottom zone combined. WT (black, n = 16 females), mutant (red, n = 16 females). * = $p < 0.01$. The box in the plot represents the 25th percentile to the 75th percentile, the line across the box represents the median, and the whiskers are the maximum and minimum data-point values. * = $p<0.05$.

the light zone; mutants first entry was 5-fold earlier than WTs (male: 8 ± 11 versus 43 ± 53 s, p = 0.02, FDR q = 0.022 and female: 5 ± 3 versus 24 ± 38, p = 0.05, not FDR significant; Figures 7D and 7E). Finally, although the number of entries into the light zone was not different (Figures 7F and 7G), the average visit time in the light zone was significantly longer in male mutants compared to male WTs (p = 0.009, FDR q = 0.025; Figure 7H), and in female mutants as compared female WTs (p = 0.038, FDR q = 0.026; Figure 7I). In sum, the results of the light-dark preference test indicate that the innate aversion to brightly illuminated spaces is suppressed in *disc1* mutants (Table 1).

disc1 mutants exhibit a preference to be part of a shoal

Zebrafish are highly social animals that form tight multimember groups (shoals).[28,55–57] To investigate social behavior in zebrafish, we used the three-chamber shoal preference test. In this assay, an adult zebrafish is placed in the center chamber of a tank that has an empty chamber on one end (asocial zone) and 5 conspecifics in the chamber on the opposite end (social zone) (Figure 8A). The behavior of the animal was recorded and social preference was assessed by quantifying the total visit time to each zone and the average time per visit to each zone. Male WT zebrafish spent more total time in the social zone as compared to the

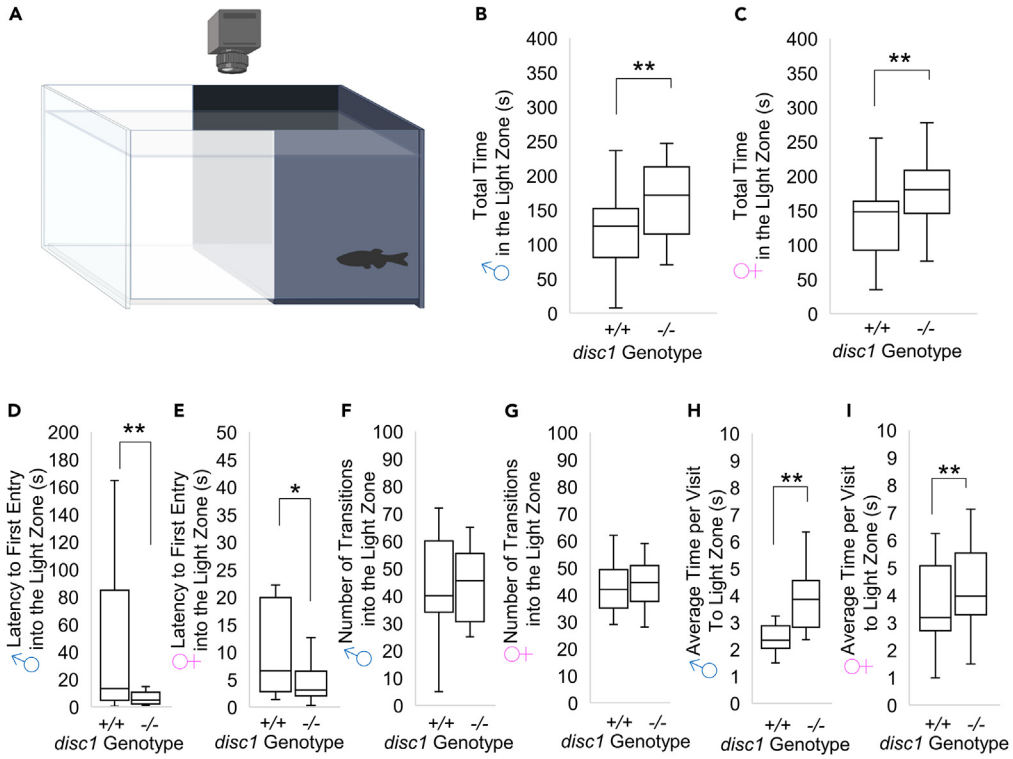

Figure 7. Adult *disc1* mutants do not exhibit scototaxis in the light-dark preference test

(A) Diagram of behavioral testing arena.

(B-G) Total time spent in the light zone (open bars) and dark zone (black bars) by WT sibling and mutant (B) males (n = 16) and (C) females (n = 16). Latency to first entry into the light zone in (D) males and (E) females. Number of transitions into the light zone in (F) males and (G) females.

(H and I) Average visit time in the light zone in (H) males and (I) females. ** = FDR significant, * = nominally significant. Data are presented as box and whisker plots. The box in the plot represents the 25th percentile to the 75th percentile, the line across the box represents the median, and the whiskers are the maximum and minimum data-point values.

asocial zone (392 ± 111 versus 39 ± 35 s, $p < 0.0001$; Figures 8B-8D). In addition, they spent significantly greater time per visit to the social zone than to the asocial zone (10.6 ± 11.3 versus 1.6 ± 0.6 s, $p < 0.0001$; Figures 8E and 8F). Male *disc1* mutants also exhibited a preference for the social zone compared to the asocial zone (365 ± 22 versus 50 ± 7 s, $p < 0.0001$; Figures 8C and 8D). They also spent significantly greater time per visit to the social zone than to the asocial zone (6.5 ± 3.0 versus 1.6 ± 0.7 s, $p < 0.0001$; Figures 8E and 8F; note the different y axis scales). These metrics of shoaling preference were not significantly different between male *disc1* WT and mutant animals (Figures 8C-8F).

Next, we tested shoal preferences in females. Female WT zebrafish exhibited significantly greater total visit time to the social zone versus the asocial zone (441 ± 156 versus 22 ± 16 s, $p < 0.0001$; Figures 8G and 8H) and greater time per visit to the social zone versus the asocial zone (17.9 ± 16.7 versus 1.1 ± 0.6 s, $p < 0.0001$; Figures 8I and 8J). Female *disc1* mutants also exhibited a preference for the social zone compared to the asocial zone. They spent significantly increased total visit time in the social versus asocial zone (487 ± 66 versus 22 ± 27 s, $p < 0.0001$; Figures 8G and 8H) and greater time per visit to the social zone versus the asocial zone (15.1 ± 17.2 versus 1.0 ± 0.5 s, $p < 0.0001$; Figures 8I and 8J). None of the metrics of shoaling preference were significantly different between female *disc1* WT and mutant animals (Figures 8G-8J).

Finally, we assessed shoal cohesion using shoals consisting of 3 males and 3 females that were placed in a single open chamber tank. We measured average-pairwise fish-fish distance, average distance to the furthest neighbor, and average distance to the nearest neighbor (Figure 8K). The average-pairwise fish-fish distance was 10% shorter in *disc1* mutant shoals as compared to WT shoals (5.5 ± 0.4 versus 6.1 ± 0.3 cm, p = 9E-06; Figure 8L). In addition, the average distance to the furthest neighbor in the shoal was 10% shorter in *disc1*

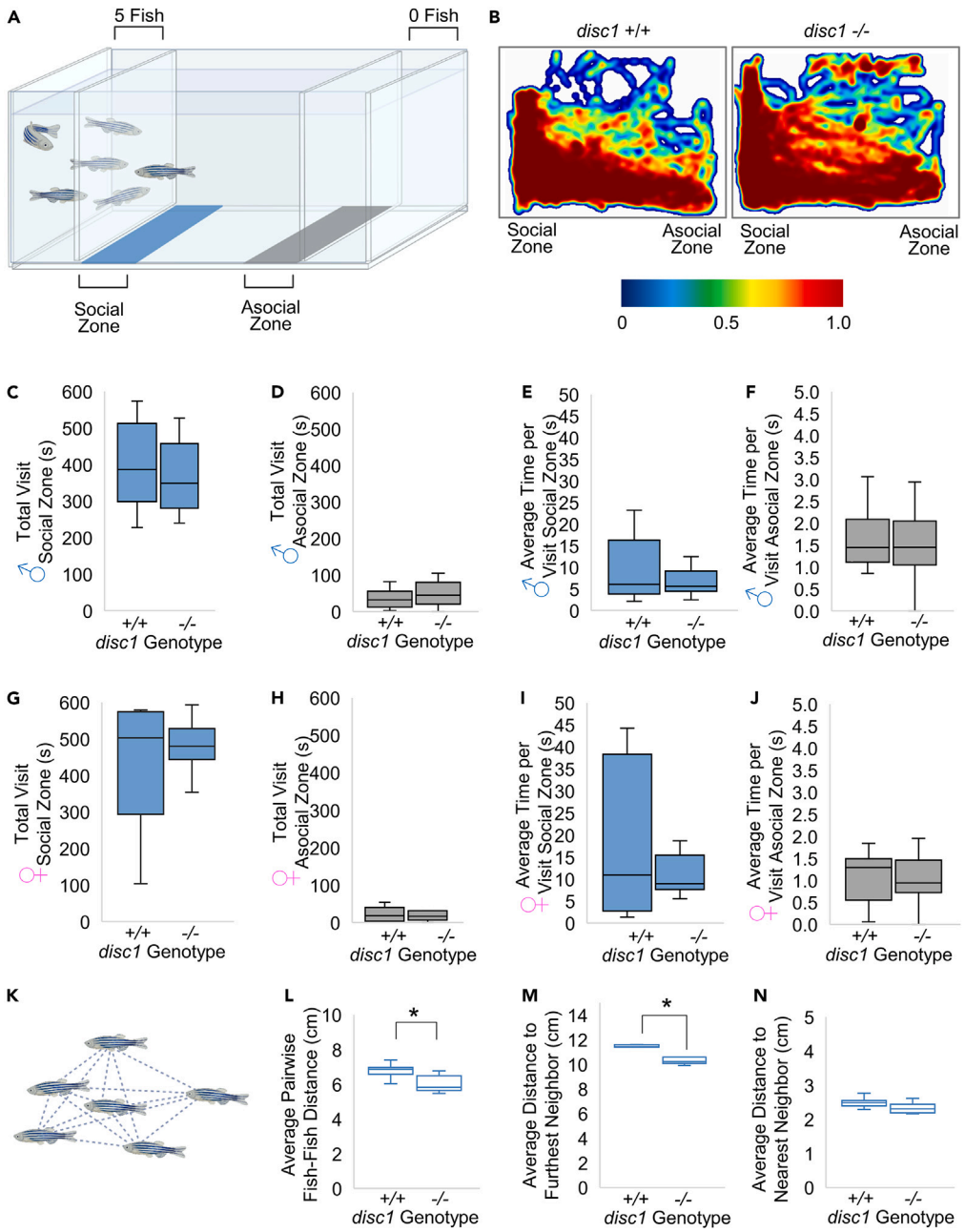

Figure 8. Adult *disc1* mutants exhibit a preference for being part of a shoal

(A) Diagram of behavioral testing arena.

(B) Heat maps depicting the amount of time spent at each location in the testing arena by a representative WT sibling and *disc1* mutant (red indicates increased time and blue indicates decreased time).

(C-F) Total visit time to the social zone, (D) total visit time to the asocial zone, (E) average time per visit to the social zone, and (F) average time per visit to the social zone in males WTs (n = 16) and male *disc1* mutants (n = 16).

(G-K) Total visit time to the asocial zone, (H) total visit time to the asocial zone, (I) average time per visit to the asocial zone, and (J) average time per visit to the asocial zone in females WTs (n = 16) and female *disc1* mutants (n = 16). (K) Pairwise interactions measured in the shoal cohesion assay (n = 18; 3 males and 3 females per shoal).

(L-N) Average pairwise fish-fish distance, (M) average distance to the furthest neighbor, and (N) average distance to the nearest neighbor. * = $p < 0.01$.

Data are presented as box and whisker plots. The box in the plot represents the 25th percentile to the 75th percentile, the line across the box represents the median, and the whiskers are the maximum and minimum data-point values.

mutant shoals as compared to WT shoals (10.3 ± 0.5 versus 11.5 ± 0.1 cm, p = 0.005; Figure 8M). There was no difference in the distance to the nearest neighbor; thus, distance to the furthest neighbor underlies the difference (Figure 8N). Together, these findings indicate that *disc1* mutants form tighter shoals.

DISCUSSION

Accurate registration of sensory information and its subsequent transformation to motor output is essential for an organism's ability to adapt to its physical environment, and to interact among conspecifics. In this study, a common correlate throughout the lifespan of *disc1* mutants was that embryos, larvae, and adults exhibit decreased responsiveness to aversive stimuli in diverse environmental contexts (Table 1). The behavioral phenotypes detected across paradigms indicated impairment in the normal processing of sensory information and stressful stimuli, in addition to response decision (sensorimotor transformation). Concordantly, whole-brain activity mapping in *disc1* mutant larvae during exposure to an acoustic sensory stimulus demonstrated that loss of *disc1* abnormally activates neurons in the pallium, cerebellum, and tectum—subregions in the central nervous system that integrate sensory input and motor output. Together these findings demonstrate that the mutation of *disc1* in zebrafish abrogates motor output in response to sensory stimuli, modulates neuronal activity in subregions involved in sensorimotor processing, and suppresses fear and anxiogenic behaviors.

As the very first behaviors emerge in embryos, behavioral defects are evident in *disc1* mutants

Neurodevelopmental abnormalities that occur *in utero* contribute to the endophenotypes observed in adult animals carrying *disc1* mutations.[13] As opposed to the *in utero* development of mammals, the external development (*ex utero*) of zebrafish allows access to all stages along the neurodevelopmental trajectory. It was intriguing to find that in our *disc1* mutant zebrafish embryos, abnormal behavioral responses to external stimuli were evident very early in embryonic development, as early as 28 hpf. One of the first behaviors to develop in zebrafish embryos is the photomotor response which is the behavioral response of dark-adapted embryos to a pulse of white light. In *disc1* embryos, the light pulse did not induce the PMR excitation phase. Although the first light pulse did not trigger PMR excitation, the second light pulse did trigger the PMR inactive phase—a reduction in motor activity (Figure 2C). This indicates that photosensation is intact,[48] and suggests that the mutants perceived the first light pulse but did not respond with a motor output. These findings were not due to an overall delay in embryonic development or to morphological defects in muscle development (Figure S2). The photomotor response occurs prior to the development of vision (24 hpf versus 74 hpf, respectively)[58,59] and thus does not require light detection by retinal cells within the eyes. Instead, the hindbrain is both necessary and sufficient for this response.[48] A light-sensing circuit that drives this motor behavior has been identified in the caudal hindbrain and consists of opsin-based photoreceptor neurons.[48] Our findings suggest that *disc1* KO zebrafish harbor defects in this sensorimotor circuit in the hindbrain and demonstrate that as the very first embryonic behaviors emerge in zebrafish, behavioral deficits are detectable in *disc1* mutants.

disc1 mutant larvae exhibit abnormal neural activity in the cerebellum, tectum, and pallium, and deficits in sensorimotor behaviors regulated by these nervous system substructures

In both mice and humans, carriers of *DISC1* mutations exhibit defects in sensorimotor behaviors, including prolonged latency time when presented with an acoustic startle stimulus and abnormal sensory gating.[10,60] Analogous assays are highly feasible in zebrafish larvae. Leveraging our high-content behavioral phenotyping platform, we next conducted a battery of 10 behavioral assays to determine the impact of combinations of visual and auditory stimuli on sensorimotor behaviors in 7-day-old *disc1* mutant larvae. *disc1* mutant larvae exhibited reduced acoustic startle as compared to sibling WTs in several behavioral assays (ASR1, ASR2, and AVSR1-3; Figure 2D). These findings are consistent with murine studies demonstrating that mutations in *disc1* result in defects in the magnitude of motor responses to sensory stimuli and defects in the rate of habituation to sensory stimuli—both of which result from deficits in neural processing of sensorimotor stimuli.[10,60] The behaviors observed in our *disc1* mutant zebrafish provide a tractable new genetic model to study the biology of sensorimotor processing pathways in the context of *disc1* deletion in an organism.

To further interrogate sensorimotor processing in the context of *disc1* deletion, we conducted whole-brain neuronal activity imaging. Brain structure and regional activity maps were generated following the delivery

of a high-magnitude acoustic stimulus and through the subsequent elicitation of motor output in *disc1* mutants and sibling controls. In response to an acoustic stimulus, there was increased bilateral activity in the pallium, cerebellum, and tectum of *disc1* mutant larvae (Figures 3 and S3). These anatomical sites are involved in the integration of sensory perception and motor control.[61] The zebrafish pallium is essential for active avoidance and motivated behavior, and contains regions homologous to the mammalian amygdala.[62–64] Thus, the acoustic startle induction of neural activity in the pallium is consistent with the pallium's role in the response to fearful stimuli. *disc1* mutants exhibit abnormal stimulus-induced neural activity in this subregion. Interestingly, in response to fearful stimuli, schizophrenic patients also exhibit altered activity patterns in the amygdala.[65]

We also observed differential neuronal activity patterns in the tectum of *disc1* mutants. The tectum in vertebrates (the superior colliculus in mammals) has an evolutionarily conserved function in processing visual-motor responses by transforming visual signals into motor responses,[66–68] in addition to processing auditory and somatosensory inputs.[69] Although less well-studied in zebrafish, in addition to processing visual stimuli, the zebrafish tectum also processes auditory and water motion stimuli.[67,70] Thus, *disc1* mutants may exhibit abnormally increased activity in the tectum in response to the auditory stimulus that we delivered in the dark, or the tectum of *disc1* may exhibit an abnormal registry of non-visual stimulus (i.e. the auditory stimulus). Moreover, the decision to approach prey or to evade a predator requires the tectum.[52,68,71] We found that the innate fear response (SLR assay) is present but abrogated in *disc1* mutant larvae as exhibited by less freezing during the first half of the stimulus as compared to wildtypes (Figure 4). These behavioral findings suggest that a predator threat stimulus (strobe light) evoked less fear in *disc1* mutants. Prior work has shown that an alarm pheromone, which indicates the presence of a predator and induces a strong fear response in zebrafish, failed to upregulate cortisol levels in *disc1* mutant larvae.[34] In response to a threat or the anticipation of a threat, cortisol-induced stress responses are activated,[72] thus it can be hypothesized that the *disc1* mutant larvae experienced decreased stress in response to a fear-inducing stimulus. Our study builds upon prior work by demonstrating that a visual predator threat stimulus (strobe light) evoked less fear in *disc1* mutants. Together with our whole-brain neuronal mapping, this implicates *disc1* in neural circuits in the pallium and tectum that impact behavioral responses to fearful stimuli, thereby providing a new entry point to study the regulation of defensive behaviors.

Early behavioral phenotypes of *disc1* larval mutants correlated with concordant phenotypes in *disc1* adults

Zebrafish engage in complex behaviors through lifespan; however, very few of the numerous neurogenic zebrafish mutant lines have undergone extensive behavioral characterization throughout key developmental stages of their life. Therefore, it is often not clear whether early surrogate phenotypes in larvae truly translate into changes in anxiety or fear in adult zebrafish. Using established paradigms of environment-induced stress, we assessed adult behaviors in *disc1* mutants. In the novel tank dive test, adult male *disc1* mutants exhibited decreased anxiety in response to the stress of a novel environment and increased engagement in exploration behavior. This was evidenced by increased distance traveled in the top zone and increased time per visit exploring the top zone (Figure 5). In a conflict-based novelty test (light-dark preference test), the innate aversion to brightly illuminated spaces (scototaxis) was suppressed in adult *disc1* mutants. *disc1* mutants spent more time in the light zone as compared to WTs, suggesting mutants did not perceive the light compartment as an aversive environment (Figure 7). Moreover, *disc1* mutants exhibited a 5-fold shorter latency to first entry into the light compartment, an indication of willingness to engage in higher-risk behavior. Cumulatively, these findings in adults are concordant with abrogated fear in *disc1* larvae in the SLR assay (Figure 4); in addition, they are concordant with the blunted responses to aversive sensory stimuli in *disc1* embryos and larvae (Figure 2).

Sex-specific effects of *disc1* in zebrafish

There were sex-specific differences in anxiogenic and exploration behaviors in *disc1* mutants. Male *disc1* mutants were less anxious than male WTs in the novel tank dive test (Figure 5), in contrast, female *disc1* mutants displayed anxiogenic behavior similar to that of female WTs (Figure 6). The novel tank dive test is a classical anxiogenic paradigm that is analogous to the open-field test used for mice. Sex-specific differences in *Disc1* mice in the open field test have been reported.[44–46] Given the extensive protein-protein interactome of Disc1,[11] sexually dimorphic behavioral phenotypes may result from sex-dependent differences in gene expression or hormone-dependent effects on GSK3β signaling in the brain.[73,74] Our data

identifying sex-specific effects of *disc1* in zebrafish in the novel tank dive test, adds new information on sexually dimorphic behaviors in zebrafish.

Effects of *disc1* on social paradigms in adult animals

In the zebrafish shoal preference test, adult male and female *disc1* mutants exhibited normal social behavior as evidenced by preferentially spending more time near the compartment with conspecifics as opposed to an empty compartment (Figure 8). This finding is consistent with a previous study, albeit in larvae, which measured shoal cohesion (distance to the nearest neighbor) in *disc1* mutant larvae[34]; under normal conditions there were no differences in larval social cohesion. However, when combined with a stressor divergent shoaling behavior emerged between mutant and WT larvae. When exposed to the pheromone Schreckstoff (a predator-stress stimulus), WT zebrafish exhibit increased shoal cohesion[75] whereas *disc1* larval mutants (5 dpf) failed to respond to the alarm stimulus, i.e. did not change shoal cohesion.[34] Interestingly, in response to the alarm stimulus, swimming speed was reduced in both WTs and mutants. This may suggest that *disc1* mutants can detect the stimulus (as evidenced by decreased swim speed) but do not process the stimulus as threatening and therefore fail to increase shoal cohesion (a protective response). Consistent with a study which used larval and juvenile age *disc1* animals (7 d.p.f. and 21 d.p.f.), as opposed to the adult age animals used in our shoaling study, tighter shoals were also observed in *disc1* mutant larvae and juveniles as compared to WTs.[19] In contrast to our findings, the García-González et al. study, which aimed to test the interaction of developmental exposure to cannabinoids in zebrafish in the context of genetic loss of *disc1*, found different results in adult WT and *disc1* mutants in the Novel Tank Diving Test.[76] Their study found that adult *disc1* mutants spent more time in the bottom of the tank in the Novel Tank Diving Test, which contradicts with our findings in the Novel Tank Diving Test. It is not clear if the differences between their findings and our findings are due to the genetic site targeted, which is known to have a strong influence on the phenotypes in mice.[10–13] Collectively this also supports our claim for the need of additional zebrafish *disc1* mutants to deconvolute the gene-environment-phenotype interactions in zebrafish, which have been far more well-established in *Disc1* mutant mice as compared to *disc1* mutant zebrafish (Jaaro-Peled, 2009, Lipina and Roder, 2014, Tomoda et al., 2016, Cash-Padgett and Jaaro-Peled, 2013. Finally, in another study that sought to stratify the dynamic motion patterns of group behavior across 90 mutant zebrafish lines, *disc1* mutant animals (6 adults) were placed in a circular open arena and their shoaling behavior was found to be dense and disordered.[77] As our shoaling assay used a 3-chambered arena and the paradigm of zone placement preference, as opposed to a single open area and the paradigm of coordinated, directional swimming used in the Tang et al. study, we also conducted a second shoaling assay. Concordantly, when placed in a single-chamber arena, our *disc1* mutants (6 adults) exhibited tighter shoal cohesion as evidenced by the reduction in average pairwise fish-fish distance (Figure 8). This paradigm requires individuals in the group to coordinate their movements as such collective group behavior requires sensory, motor, and integrative processes. Therefore, this collective group behavior assesses sensorimotor transformations in addition to social interactions. In the future, it will be interesting to examine the effects of strobe light, acoustic startle, or other threatening stimuli on shoaling behaviors in our *disc1* mutant zebrafish using both the 3-chamber and single-chamber paradigms.

Limitations and future directions

Our study does have some limitations. First, increased impulsivity, engaging in risk-taking, and decreased anxiety are challenging to distinguish in animal models, and the novel tank diving assay and light-dark preference test have been used to study all these behaviors. Second, the identity of the neuronal cell types that are activated in *disc1* mutant tectum and pallium are not known. Future investigations using the ablation of targeted neurons or light-based optogenetic manipulations will aid in the identification of these neural circuits. Third, the phenotypes detected may indicate impairment in the processing of sensory information, in the integration of sensory and motor outputs, or in the response decision. Future investigations are required to distinguish between these possibilities. Fourth, Disc1 plays a role in early neurodevelopment processes including neuronal progenitor cell proliferation, migration, and differentiation. Using the Z-brain atlas to conduct structural analysis, no malformations occurred during the development of the central nervous system in *disc1* mutants. Future experiments examining more nuanced neurodevelopmental processes are needed to fully assess if proliferation, migration, or differentiation processes are altered and if these affect the behaviors in *disc1* mutants (Table 1). In addition, given zebrafish allow for easy access to all stages along the neurodevelopmental trajectory: gastrulation, embryonic, and larval stages of neurodevelopment—all occurring over a 6-day period, in the future, subjecting *disc1* mutant embryos to perturbations between 0 and 6 dpf and subsequently raising them to adulthood will aid in elucidating the

molecular interactions between environment, neurodevelopment, and adult behaviors. Finally, in future studies, this *disc1* genetic model will be a tractable new tool for high-throughput behavioral screens aimed at small molecule drug discovery.[78] Several behavioral phenotypes identified in this study can be leveraged endpoints in high-throughput chemical screens in *disc1* mutants (Figures 2C, 2D, 4A, and 4B). Previously, we have successfully leveraged "behavioral bar coding" in the photomotor response assay, automated multiplex sensorimotor response assay, and strobe light response assay to identify novel neuroactive small molecules.[23–25] Thus having identified, in this study, the embryonic and larval sensorimotor phenotypes in our *disc1* mutants (Figures 2C, 2D, 4A, and 4B)—in the exact same behavioral phenotyping platforms that are used for high-content screening—we set the stage for large-scale small molecule screens aimed at discovering novel pharmaceuticals to reverse the sensorimotor defects in carriers of *disc1* mutations.

Conclusions

Sensory input and motor systems are tightly intertwined, and adapting to environmental stimuli requires their coordinated integration. Cumulatively, our findings indicate that *disc1* embryos and larvae exhibit aberrant global motor outputs in response to sensory stimuli, while *disc1* adults exhibit reduced anxiogenic behaviors and increased risk-taking behaviors in novel paradigms. Our data also provide novel insights into the functional role of *disc1* in the brain by demonstrating that loss of *disc1* leads to abnormal neuronal activity in the cerebellum, tectum, and pallium. These findings suggest new lines of investigation that could be undertaken in *disc1* zebrafish aimed at investigating the impact of *disc1* on sensorimotor neural circuits. In addition to interrogating gene function, this model provides opportunities to test potential therapies in high-throughput behavioral assays.

STAR★METHODS

Detailed methods are provided in the online version of this paper and include the following:

- KEY RESOURCES TABLE
- RESOURCE AVAILABILITY
  - Lead contact
  - Materials availability
  - Data and code availability
- EXPERIMENTAL MODEL AND SUBJECT DETAILS
  - Animals
- METHOD DETAILS
  - Western blot
  - Embryo and larval behavioral phenotyping
  - Photomotor response
  - Somite counting
  - F-actin staining
  - Automated multiplex sensorimotor response assay
  - Whole-brain activity and morphology
  - Strobe light response assay
  - Behavioral testing room and adult fish handling
  - Novel tank diving test
  - Light-dark preference test
  - Three chamber shoaling preference test
  - Shoal cohesion
- QUANTIFICATION AND STATISTICAL ANALYSIS

SUPPLEMENTAL INFORMATION

Supplemental information can be found online at https://doi.org/10.1016/j.isci.2023.107099.

ACKNOWLEDGMENTS

We thank the BIDMC Zebrafish Core Facility for assistance. We would like to thank Drs. Dheeraj Malhotra, Martin Ebeling, Marco Berrera, Theo Dinklo, Will Spooren, and Anirvan Ghosh (all at Hoffmann – La Roche during the work) for scientific advice/guidance.

AUTHOR CONTRIBUTIONS

BRP, CB, DLH, and ST conducted the experiments and analyzed the data. EPP, MRE, RTP, and AKN conceived the project and supervised the work. All authors contributed to the ideas of the project and the final article. AKN wrote the original draft of the article. All authors revised the article. MRE, RTP, and AKN provided the resources for the project.

DECLARATION OF INTERESTS

This work was supported, in part, by a sponsored research agreement with Hoffmann-La Roche.

INCLUSION AND DIVERSITY

We support inclusive, diverse, and equitable conduct of research.

Received: September 2, 2022
Revised: March 27, 2023
Accepted: June 8, 2023
Published: June 14, 2023

REFERENCES

1. Jacobs, P.A., Brunton, M., Frackiewicz, A., Newton, M., Cook, P.J.L., and Robson, E.B. (1970). Studies on a family with three cytogenetic markers. Ann. Hum. Genet. *33*, 325–336. https://doi.org/10.1111/j.1469-1809.1970.tb01658.x.

2. St Clair, D., Blackwood, D., Muir, W., Carothers, A., Walker, M., Spowart, G., Gosden, C., and Evans, H.J. (1990). Association within a family of a balanced autosomal translocation with major mental illness. Lancet *336*, 13–16.

3. Kilpinen, H., Ylisaukko-Oja, T., Hennah, W., Palo, O.M., Varilo, T., Vanhala, R., Nieminen-von Wendt, T., von Wendt, L., Paunio, T., and Peltonen, L. (2008). Association of DISC1 with autism and Asperger syndrome. Mol. Psychiatr. *13*, 187–196. https://doi.org/10.1038/sj.mp.4002031.

4. Jacobsen, K.K., Halmøy, A., Sánchez-Mora, C., Ramos-Quiroga, J.A., Cormand, B., Haavik, J., and Johansson, S. (2013). DISC1 in adult ADHD patients: an association study in two European samples. Am. J. Med. Genet. B Neuropsychiatr. Genet. *162B*, 227–234. https://doi.org/10.1002/ajmg.b.32136.

5. Hennah, W., Thomson, P., Peltonen, L., and Porteous, D. (2006). Genes and schizophrenia: beyond schizophrenia: the role of DISC1 in major mental illness. Schizophr. Bull. *32*, 409–416. https://doi.org/10.1093/schbul/sbj079.

6. Millar, J.K., Wilson-Annan, J.C., Anderson, S., Christie, S., Taylor, M.S., Semple, C.A., Devon, R.S., St Clair, D.M., Muir, W.J., Blackwood, D.H., and Porteous, D.J. (2000). Disruption of two novel genes by a translocation co-segregating with schizophrenia. Hum. Mol. Genet. *9*, 1415–1423.

7. Schosser, A., Gaysina, D., Cohen-Woods, S., Chow, P.C., Martucci, L., Craddock, N., Farmer, A., Korszun, A., Gunasinghe, C., Gray, J., et al. (2010). Association of DISC1 and TSNAX genes and affective disorders in the depression case-control (DeCC) and bipolar affective case-control (BACCS) studies. Mol. Psychiatr. *15*, 844–849. https://doi.org/10.1038/mp.2009.21.

8. Thomson, P.A., Malavasi, E.L.V., Grünewald, E., Soares, D.C., Borkowska, M., and Millar, J.K. (2013). DISC1 genetics, biology and psychiatric illness. Front. Biol. *8*, 1–31. https://doi.org/10.1007/s11515-012-1254-7.

9. Brandon, N.J., and Sawa, A. (2011). Linking neurodevelopmental and synaptic theories of mental illness through DISC1. Nat. Rev. Neurosci. *12*, 707–722. https://doi.org/10.1038/nrn3120.

10. Jaaro-Peled, H. (2009). Gene models of schizophrenia: DISC1 mouse models. Prog. Brain Res. *179*, 75–86. https://doi.org/10.1016/S0079-6123(09)17909-8.

11. Lipina, T.V., and Roder, J.C. (2014). Disrupted-In-Schizophrenia-1 (DISC1) interactome and mental disorders: impact of mouse models. Neurosci. Biobehav. Rev. *45*, 271–294. https://doi.org/10.1016/j.neubiorev.2014.07.001.

12. Tomoda, T., Sumitomo, A., Jaaro-Peled, H., and Sawa, A. (2016). Utility and validity of DISC1 mouse models in biological psychiatry. Neuroscience *321*, 99–107. https://doi.org/10.1016/j.neuroscience.2015.12.061.

13. Cash-Padgett, T., and Jaaro-Peled, H. (2013). DISC1 mouse models as a tool to decipher gene-environment interactions in psychiatric disorders. Front. Behav. Neurosci. *7*, 113. https://doi.org/10.3389/fnbeh.2013.00113.

14. Gerlai, R. (2012). Using zebrafish to unravel the genetics of complex brain disorders. Curr. Top. Behav. Neurosci. *12*, 3–24. https://doi.org/10.1007/7854_2011_180.

15. Kalueff, A.V., Stewart, A.M., and Gerlai, R. (2014). Zebrafish as an emerging model for studying complex brain disorders. Trends Pharmacol. Sci. *35*, 63–75. https://doi.org/10.1016/j.tips.2013.12.002 S0165-6147(13)00229-0.

16. Kalueff, A.V., Gebhardt, M., Stewart, A.M., Cachat, J.M., Brimmer, M., Chawla, J.S., Craddock, C., Kyzar, E.J., Roth, A., Landsman, S., et al. (2013). Towards a comprehensive catalog of zebrafish behavior 1.0 and beyond. Zebrafish *10*, 70–86. https://doi.org/10.1089/zeb.2012.0861.

17. Tropepe, V., and Sive, H.L. (2003). Can zebrafish be used as a model to study the neurodevelopmental causes of autism? Gene Brain Behav. *2*, 268–281.

18. Bolton, A.D., Haesemeyer, M., Jordi, J., Schaechtle, U., Saad, F.A., Mansinghka, V.K., Tenenbaum, J.B., and Engert, F. (2019). Elements of a stochastic 3D prediction engine in larval zebrafish prey capture. Elife *8*, e51975. https://doi.org/10.7554/eLife.51975.

19. Harpaz, R., Aspiras, A.C., Chambule, S., Tseng, S., Bind, M.A., Engert, F., Fishman, M.C., and Bahl, A. (2021). Collective behavior emerges from genetically controlled simple behavioral motifs in zebrafish. Sci. Adv. *7*, eabi7460. https://doi.org/10.1126/sciadv.abi7460.

20. Xu, J., Casanave, R., and Guo, S. (2021). Larval zebrafish display dynamic learning of aversive stimuli in a constant visual surrounding. Learn. Mem. *28*, 228–238. https://doi.org/10.1101/lm.053425.121.

21. Burgess, H.A., and Granato, M. (2007). Sensorimotor gating in larval zebrafish. J. Neurosci. *27*, 4984–4994. https://doi.org/10.1523/JNEUROSCI.0615-07.2007.

22. Wolman, M.A., Jain, R.A., Liss, L., and Granato, M. (2011). Chemical modulation of memory formation in larval zebrafish. Proc. Natl. Acad. Sci. USA *108*, 15468–15473. https://doi.org/10.1073/pnas.1107156108.

23. Kokel, D., Bryan, J., Laggner, C., White, R., Cheung, C.Y.J., Mateus, R., Healey, D., Kim, S., Werdich, A.A., Haggarty, S.J., et al. (2010).

Rapid behavior-based identification of neuroactive small molecules in the zebrafish. Nat. Chem. Biol. *6*, 231–237. https://doi.org/10.1038/nchembio.307.

24. Rennekamp, A.J., Huang, X.P., Wang, Y., Patel, S., Lorello, P.J., Cade, L., Gonzales, A.P.W., Yeh, J.R.J., Caldarone, B.J., Roth, B.L., et al. (2016). sigma1 receptor ligands control a switch between passive and active threat responses. Nat. Chem. Biol. *12*, 552–558. https://doi.org/10.1038/nchembio.2089 nchembio.2089.

25. Bruni, G., Rennekamp, A.J., Velenich, A., McCarroll, M., Gendelev, L., Fertsch, E., Taylor, J., Lakhani, P., Lensen, D., Evron, T., et al. (2016). Zebrafish behavioral profiling identifies multitarget antipsychotic-like compounds. Nat. Chem. Biol. *12*, 559–566. https://doi.org/10.1038/nchembio.2097 nchembio.2097.

26. Wong, K.K., Filatov, S., Kibblewhite, D.J., Elkhayat, S., Tien, D., Roy, S., Goodspeed, J., Suciu, C., Tan, J., Grimes, C., et al. (2010). Analyzing habituation responses to novelty in zebrafish (Danio rerio). Laryngoscope *120*, 450–453. https://doi.org/10.1016/j.bbr.2009.12.023 S0166-4328(09)00749-9.

27. Maximino, C., Marques de Brito, T., Dias, C.A.G.D.M., Gouveia, A., Jr., and Morato, S. (2010). Scototaxis as anxiety-like behavior in fish. Nat. Protoc. *5*, 209–216. https://doi.org/10.1038/nprot.2009.225.

28. Saverino, C., and Gerlai, R. (2008). The social zebrafish: behavioral responses to conspecific, heterospecific, and computer animated fish. Behav. Brain Res. *191*, 77–87. https://doi.org/10.1016/j.bbr.2008.03.013.

29. Miller, N., and Gerlai, R. (2007). Quantification of shoaling behaviour in zebrafish (Danio rerio). Behav. Brain Res. *184*, 157–166. https://doi.org/10.1016/j.bbr.2007.07.007.

30. De Rienzo, G., Bishop, J.A., Mao, Y., Pan, L., Ma, T.P., Moens, C.B., Tsai, L.H., and Sive, H. (2011). Disc1 regulates both beta-catenin-mediated and noncanonical Wnt signaling during vertebrate embryogenesis. Faseb. J. *25*, 4184–4197. https://doi.org/10.1096/fj.11-186239 fj.11-186239.

31. Wood, J.D., Bonath, F., Kumar, S., Ross, C.A., and Cunliffe, V.T. (2009). Disrupted-in-schizophrenia 1 and neuregulin 1 are required for the specification of oligodendrocytes and neurones in the zebrafish brain. Hum. Mol. Genet. *18*, 391–404. https://doi.org/10.1093/hmg/ddn361 ddn361.

32. Drerup, C.M., Wiora, H.M., Topczewski, J., and Morris, J.A. (2009). Disc1 regulates foxd3 and sox10 expression, affecting neural crest migration and differentiation. Development *136*, 2623–2632. https://doi.org/10.1242/dev.030577 dev.030577.

33. Singh, K.K., De Rienzo, G., Drane, L., Mao, Y., Flood, Z., Madison, J., Ferreira, M., Bergen, S., King, C., Sklar, P., et al. (2011). Common DISC1 polymorphisms disrupt Wnt/GSK3beta signaling and brain development. Neuron *72*, 545–558. https://doi.org/10.1016/j.neuron.2011.09.030.

34. Eachus, H., Bright, C., Cunliffe, V.T., Placzek, M., Wood, J.D., and Watt, P.J. (2017). Disrupted-in-Schizophrenia-1 is essential for normal hypothalamic-pituitary-interrenal (HPI) axis function. Hum. Mol. Genet. *26*, 1992–2005. https://doi.org/10.1093/hmg/ddx076.

35. Morris, J.A. (2009). Zebrafish: a model system to examine the neurodevelopmental basis of schizophrenia. Prog. Brain Res. *179*, 97–106. https://doi.org/10.1016/S0079-6123(09)17911-6.

36. Boyd, P.J., Cunliffe, V.T., Roy, S., and Wood, J.D. (2015). Sonic hedgehog functions upstream of disrupted-in-schizophrenia 1 (disc1): implications for mental illness. Biol. Open *4*, 1336–1343. https://doi.org/10.1242/bio.012005.

37. Clapcote, S.J., Lipina, T.V., Millar, J.K., Mackie, S., Christie, S., Ogawa, F., Lerch, J.P., Trimble, K., Uchiyama, M., Sakuraba, Y., et al. (2007). Behavioral phenotypes of Disc1 missense mutations in mice. Neuron *54*, 387–402. https://doi.org/10.1016/j.neuron.2007.04.015.

38. Hikida, T., Jaaro-Peled, H., Seshadri, S., Oishi, K., Hookway, C., Kong, S., Wu, D., Xue, R., Andradé, M., Tankou, S., et al. (2007). Dominant-negative DISC1 transgenic mice display schizophrenia-associated phenotypes detected by measures translatable to humans. Proc. Natl. Acad. Sci. USA *104*, 14501–14506. https://doi.org/10.1073/pnas.0704774104.

39. Johnson, A.W., Jaaro-Peled, H., Shahani, N., Sedlak, T.W., Zoubovsky, S., Burruss, D., Emiliani, F., Sawa, A., and Gallagher, M. (2013). Cognitive and motivational deficits together with prefrontal oxidative stress in a mouse model for neuropsychiatric illness. Proc. Natl. Acad. Sci. USA *110*, 12462–12467. https://doi.org/10.1073/pnas.1307925110.

40. Kuroda, K., Yamada, S., Tanaka, M., Iizuka, M., Yano, H., Mori, D., Tsuboi, D., Nishioka, T., Namba, T., Iizuka, Y., et al. (2011). Behavioral alterations associated with targeted disruption of exons 2 and 3 of the Disc1 gene in the mouse. Hum. Mol. Genet. *20*, 4666–4683. https://doi.org/10.1093/hmg/ddr400.

41. Lipina, T.V., Niwa, M., Jaaro-Peled, H., Fletcher, P.J., Seeman, P., Sawa, A., and Roder, J.C. (2010). Enhanced dopamine function in DISC1-L100P mutant mice: implications for schizophrenia. Gene Brain Behav. *9*, 777–789. https://doi.org/10.1111/j.1601-183X.2010.00615.x.

42. Kvajo, M., McKellar, H., Arguello, P.A., Drew, L.J., Moore, H., MacDermott, A.B., Karayiorgou, M., and Gogos, J.A. (2008). A mutation in mouse Disc1 that models a schizophrenia risk allele leads to specific alterations in neuronal architecture and cognition. Proc. Natl. Acad. Sci. USA *105*, 7076–7081. https://doi.org/10.1073/pnas.0802615105.

43. Koike, H., Arguello, P.A., Kvajo, M., Karayiorgou, M., and Gogos, J.A. (2006). Disc1 is mutated in the 129S6/SvEv strain and modulates working memory in mice. Proc. Natl. Acad. Sci. USA *103*, 3693–3697. https://doi.org/10.1073/pnas.0511189103.

44. Dachtler, J., Elliott, C., Rodgers, R.J., Baillie, G.S., and Clapcote, S.J. (2016). Missense mutation in DISC1 C-terminal coiled-coil has GSK3beta signaling and sex-dependent behavioral effects in mice. Sci. Rep. *6*, 18748. https://doi.org/10.1038/srep18748.

45. Dachtler, J., and Fox, K. (2017). Do cortical plasticity mechanisms differ between males and females? J. Neurosci. Res. *95*, 518–526. https://doi.org/10.1002/jnr.23850.

46. Dahoun, T., Trossbach, S.V., Brandon, N.J., Korth, C., and Howes, O.D. (2017). The impact of Disrupted-in-Schizophrenia 1 (DISC1) on the dopaminergic system: a systematic review. Transl. Psychiatry *7*, e1015. https://doi.org/10.1038/tp.2016.282.

47. Soares, D.C., Carlyle, B.C., Bradshaw, N.J., and Porteous, D.J. (2011). DISC1: Structure, Function, and Therapeutic Potential for Major Mental Illness. ACS Chem. Neurosci. *2*, 609–632. https://doi.org/10.1021/cn200062k.

48. Kokel, D., Dunn, T.W., Ahrens, M.B., Alshut, R., Cheung, C.Y.J., Saint-Amant, L., Bruni, G., Mateus, R., van Ham, T.J., Shiraki, T., et al. (2013). Identification of nonvisual photomotor response cells in the vertebrate hindbrain. J. Neurosci. *33*, 3834–3843. https://doi.org/10.1523/JNEUROSCI.3689-12.2013.

49. Randlett, O., Wee, C.L., Naumann, E.A., Nnaemeka, O., Schoppik, D., Fitzgerald, J.E., Portugues, R., Lacoste, A.M.B., Riegler, C., Engert, F., and Schier, A.F. (2015). Whole-brain activity mapping onto a zebrafish brain atlas. Nat. Methods *12*, 1039–1046. https://doi.org/10.1038/nmeth.3581.

50. Jefferis, G.S.X.E., Potter, C.J., Chan, A.M., Marin, E.C., Rohlfing, T., Maurer, C.R., Jr., and Luo, L. (2007). Comprehensive maps of Drosophila higher olfactory centers: spatially segregated fruit and pheromone representation. Cell *128*, 1187–1203. https://doi.org/10.1016/j.cell.2007.01.040.

51. Thyme, S.B., Pieper, L.M., Li, E.H., Pandey, S., Wang, Y., Morris, N.S., Sha, C., Choi, J.W., Herrera, K.J., Soucy, E.R., et al. (2019). Phenotypic Landscape of Schizophrenia-Associated Genes Defines Candidates and Their Shared Functions. Cell *177*, 478–491.e20. https://doi.org/10.1016/j.cell.2019.01.048.

52. Temizer, I., Donovan, J.C., Baier, H., and Semmelhack, J.L. (2015). A Visual Pathway for Looming-Evoked Escape in Larval Zebrafish. Curr. Biol. *25*, 1823–1834. https://doi.org/10.1016/j.cub.2015.06.002.

53. Colwill, R.M., and Creton, R. (2011). Imaging escape and avoidance behavior in zebrafish larvae. Rev. Neurosci. *22*, 63–73. https://doi.org/10.1515/RNS.2011.008.

54. Kysil, E.V., Meshalkina, D.A., Frick, E.E., Echevarria, D.J., Rosemberg, D.B., Maximino, C., Lima, M.G., Abreu, M.S., Giacomini, A.C., Barcellos, L.J.G., et al. (2017). Comparative Analyses of Zebrafish Anxiety-Like Behavior Using Conflict-Based Novelty Tests. Zebrafish

14, 197–208. https://doi.org/10.1089/zeb.2016.1415.

55. Engeszer, R.E., Patterson, L.B., Rao, A.A., and Parichy, D.M. (2007). Zebrafish in the wild: a review of natural history and new notes from the field. Zebrafish *4*, 21–40. https://doi.org/10.1089/zeb.2006.9997.

56. Buske, C., and Gerlai, R. (2011). Shoaling develops with age in Zebrafish (Danio rerio). Prog. Neuro-Psychopharmacol. Biol. Psychiatry *35*, 1409–1415. https://doi.org/10.1016/j.pnpbp.2010.09.003.

57. Geng, Y., and Peterson, R.T. (2019). The zebrafish subcortical social brain as a model for studying social behavior disorders. Dis. Model. Mech. *12*, dmm039446. https://doi.org/10.1242/dmm.039446.

58. Easter, S.S., Jr., and Nicola, G.N. (1997). The development of eye movements in the zebrafish (Danio rerio). Dev. Psychobiol. *31*, 267–276. https://doi.org/10.1002/(sici)1098-2302(199712)31:4<267::aid-dev4>3.0.co;2-p.

59. Schmitt, E.A., and Dowling, J.E. (1999). Early retinal development in the zebrafish, Danio rerio: light and electron microscopic analyses. J. Comp. Neurol. *404*, 515–536.

60. Smith, A.K., Jovanovic, T., Kilaru, V., Lori, A., Gensler, L., Lee, S.S., Norrholm, S.D., Massa, N., Cuthbert, B., Bradley, B., et al. (2017). A Gene-Based Analysis of Acoustic Startle Latency. Front. Psychiatr. *8*, 117. https://doi.org/10.3389/fpsyt.2017.00117.

61. Bae, Y.K., Kani, S., Shimizu, T., Tanabe, K., Nojima, H., Kimura, Y., Higashijima, S.i., and Hibi, M. (2009). Anatomy of zebrafish cerebellum and screen for mutations affecting its development. Dev. Biol. *330*, 406–426. https://doi.org/10.1016/j.ydbio.2009.04.013.

62. Perathoner, S., Cordero-Maldonado, M.L., and Crawford, A.D. (2016). Potential of zebrafish as a model for exploring the role of the amygdala in emotional memory and motivational behavior. J. Neurosci. Res. *94*, 445–462. https://doi.org/10.1002/jnr.23712.

63. Aoki, T., Kinoshita, M., Aoki, R., Agetsuma, M., Aizawa, H., Yamazaki, M., Takahoko, M., Amo, R., Arata, A., Higashijima, S.i., et al. (2013). Imaging of neural ensemble for the retrieval of a learned behavioral program. Neuron *78*, 881–894. https://doi.org/10.1016/j.neuron.2013.04.009.

64. von Trotha, J.W., Vernier, P., and Bally-Cuif, L. (2014). Emotions and motivated behavior converge on an amygdala-like structure in the zebrafish. Eur. J. Neurosci. *40*, 3302–3315. https://doi.org/10.1111/ejn.12692.

65. Rasetti, R., Mattay, V.S., Wiedholz, L.M., Kolachana, B.S., Hariri, A.R., Callicott, J.H., Meyer-Lindenberg, A., and Weinberger, D.R. (2009). Evidence that altered amygdala activity in schizophrenia is related to clinical state and not genetic risk. Am. J. Psychiatr. *166*, 216–225. https://doi.org/10.1176/appi.ajp.2008.08020261.

66. Suzuki, D.G., Pérez-Fernández, J., Wibble, T., Kardamakis, A.A., and Grillner, S. (2019). The role of the optic tectum for visually evoked orienting and evasive movements. Proc. Natl. Acad. Sci. USA *116*, 15272–15281. https://doi.org/10.1073/pnas.1907962116.

67. Thompson, A.W., Vanwalleghem, G.C., Heap, L.A., and Scott, E.K. (2016). Functional Profiles of Visual-Auditory-and Water Flow-Responsive Neurons in the Zebrafish Tectum. Curr. Biol. *26*, 743–754. https://doi.org/10.1016/j.cub.2016.01.041.

68. Barker, A.J., and Baier, H. (2015). Sensorimotor decision making in the zebrafish tectum. Curr. Biol. *25*, 2804–2814. https://doi.org/10.1016/j.cub.2015.09.055.

69. Drager, U.C., and Hubel, D.H. (1975). Physiology of visual cells in mouse superior colliculus and correlation with somatosensory and auditory input. Nature *253*, 203–204. https://doi.org/10.1038/253203a0.

70. Pietri, T., Romano, S.A., Pérez-Schuster, V., Boulanger-Weill, J., Candat, V., and Sumbre, G. (2017). The Emergence of the Spatial Structure of Tectal Spontaneous Activity Is Independent of Visual Inputs. Cell Rep. *19*, 939–948. https://doi.org/10.1016/j.celrep.2017.04.015.

71. Helmbrecht, T.O., Dal Maschio, M., Donovan, J.C., Koutsouli, S., and Baier, H. (2018). Topography of a Visuomotor Transformation. Neuron *100*, 1429–1445.e4. https://doi.org/10.1016/j.neuron.2018.10.021.

72. Egan, R.J., Bergner, C.L., Hart, P.C., Cachat, J.M., Canavello, P.R., Elegante, M.F., Elkhayat, S.I., Bartels, B.K., Tien, A.K., Tien, D.H., et al. (2009). Understanding behavioral and physiological phenotypes of stress and anxiety in zebrafish. Behav. Brain Res. *205*, 38–44. https://doi.org/10.1016/j.bbr.2009.06.022.

73. Wandosell, F., Varea, O., Arevalo, M.A., and Garcia-Segura, L.M. (2012). Oestradiol regulates beta-catenin-mediated transcription in neurones. J. Neuroendocrinol. *24*, 191–194. https://doi.org/10.1111/j.1365-2826.2011.02186.x.

74. Ostrer, H. (2001). Invited review: sex-based differences in gene expression. J. Appl. Physiol. *91*, 2384–2388. https://doi.org/10.1152/jappl.2001.91.5.2384.

75. Speedie, N., and Gerlai, R. (2008). Alarm substance induced behavioral responses in zebrafish (Danio rerio). Behav. Brain Res. *188*, 168–177. https://doi.org/10.1016/j.bbr.2007.10.031.

76. García-González, J., de Quadros, B., Havelange, W., Brock, A.J., and Brennan, C.H. (2021). Behavioral Effects of Developmental Exposure to JWH-018 in Wild-Type and Disrupted in Schizophrenia 1 (disc1) Mutant Zebrafish. Biomolecules *11*, 319. https://doi.org/10.3390/biom11020319.

77. Tang, W., Davidson, J.D., Zhang, G., Conen, K.E., Fang, J., Serluca, F., Li, J., Xiong, X., Coble, M., Tsai, T., et al. (2020). Genetic Control of Collective Behavior in Zebrafish. iScience *23*, 100942. https://doi.org/10.1016/j.isci.2020.100942.

78. Sotiropoulos, M.G., Poulogiannopoulou, E., Delis, F., Dalla, C., Antoniou, K., and Kokras, N. (2021). Innovative screening models for the discovery of new schizophrenia drug therapies: an integrated approach. Expet Opin. Drug Discov. *16*, 791–806. https://doi.org/10.1080/17460441.2021.1877657.

79. Kimmel, C.B., Ballard, W.W., Kimmel, S.R., Ullmann, B., and Schilling, T.F. (1995). Stages of embryonic development of the zebrafish. Dev. Dynam. *203*, 253–310. https://doi.org/10.1002/aja.1002030302.

80. Stickney, H.L., Barresi, M.J., and Devoto, S.H. (2000). Somite development in zebrafish. Dev. Dynam. *219*, 287–303. https://doi.org/10.1002/1097-0177(2000)9999:9999<::AID-DVDY1065>3.0.CO;2-A.

STAR★METHODS

KEY RESOURCES TABLE

REAGENT or RESOURCE	SOURCE	IDENTIFIER
Antibodies		
Alexa Fluor 594 Phalloidin	Invitrogen	A12381
Anti-DISC1	Abcam	ab191455
Anti-phosphorylated-ERK	Cell Signaling	43700
Anti-total-ERK	Cell Signaling	4696
Experimental models: Organisms/strains		
disc1-Δ20 mutant zebrafish	This paper	ZDB-ALT-210308-1
disc1-Δ10 mutant zebrafish	This paper	N/A
cacna1a mutant zebrafish	This paper	N/A
Oligonucleotides		
disc1-Δ20 TGCAGCTGTCATGGGTCATT (forward-6FAM) CGAAACCCTCTGTCAGCCAT (reverse)	This paper	N/A
disc1-Δ10 CTGTAATCTGTGCTCAACAGGTG (forward-6FAM) AGTTCTGGGTGAATAGCATGTGT (reverse)	This paper	N/A
cacna1a ACAAAACCGCACAGAACAGC (forward-6FAM) and ACGATATTGATGCACGCCCT (reverse)	This paper	N/A
Software and algorithms		
Actual-Track Video Tracking Software	Actual Analytics, Edinburgh, UK	N/A
Zebrabox Software	ViewPoint	N/A
Z-Brain	PMID: 26778924	http://engertlab.fas.harvard.edu/Z-Brain/

RESOURCE AVAILABILITY

Lead contact

Further information and requests for resources and reagents should be directed to and will be fulfilled by the lead contact, Anjali Nath (anath1@bidmc.harvard.edu).

Materials availability

The *disc1*-Δ10 mutant line has been submitted to and will be distributed by ZIRC following publication (https://zfin.org ZFIN ID: ZDB-ALT-210308-1).

Data and code availability

All data and code can be requested from the lead contact. This paper does not report original code. Any additional information required to reanalyze the data reported in this paper is available from the lead contact upon request.

EXPERIMENTAL MODEL AND SUBJECT DETAILS

Animals

Zebrafish were maintained and embryos were obtained according to standard fish husbandry protocols. *disc1* mutant zebrafish were generated in *Tübingen* zebrafish by CRISPR-Cas9 mediated genome editing. A site in exon 2 of the zebrafish *disc1* gene (Ensembl: ENSDARG00000021895) was targeted using the following gRNA: 5′ GGCTCAGACCGCATGTATCCGGG 3′ (the PAM nucleotides are underlined). At the 1-cell stage ~100 ng/μL of sgRNA and 150 ng/μL of Cas9 mRNA were co-injected. The *disc1* mutant line

generated has a 20-base pair deletion starting at base pair position +129. Genome edits were confirmed by Sanger Sequencing. Founders were outcrossed to establish the F1 generation. F2 generation fish were genotyped using the following PCR primers: TGCAGCTGTCATGGGTCATT (forward-6FAM) and CGAAACCCTCTGTCAGCCAT (reverse). The PCR products were subjected to DNA fragment analysis using the ABI 3730xl DNA Analyzer. The wildtypes exhibit a 345 base pair peak whereas the homozygous knockouts exhibit a 325 base pair peak. In addition to the *disc1*-Δ20 mutant, a second *disc1* mutant was generated (*disc1*-Δ10 mutant) using the following gRNA: 5′ GGCGAGAAATGGCTGACAGAGGG 3′ (the PAM nucleotides are underlined). The following PCR primers were used: CTGTAATCTGTGCTCAACA GGTG (forward-6FAM) and AGTTCTGGGTGAATAGCATGTGT (reverse). Note, the *disc1*-Δ20 mutant was used for all studies except for Figure S6 which used the *disc1*-Δ10 mutant. The *cacna1c* mutant was generated by targeting a site in exon 2 of the *cacna1* gene (Ensembl: ENSDARG00000008398) using the following gRNA: 5′ GGCTGCCTGCCAACTAAGGG 3′ (the PAM nucleotides are underlined). The following PCR primers were used: ACAAAACCGCACAGAACAGC (forward-6FAM) and ACGATATTGATGCAC GCCCT (reverse). All methods were carried out in accordance with the regulations and guidelines of the Animal Welfare Act and the American Association for Accreditation of Laboratory Animal Care. All experimental protocols were approved by the IACUC committee at MGH and BIDMC. Zebrafish embryos and larvae were housed in 150 mm Petri dishes at a density of <150 per dish. They were grown at 28°C in HEPES-buffered Tübingen E3 medium inside light/dark cycle incubators (14 h light/10 h dark). Behavioral experiments were conducted on 28 hpf to 7 dpf animals; at this developmental stage the sex of the organism has not yet been determined. Behavioral testing occurred between 9 a.m. and 5 p.m. in a behavioral testing room at 28°C.

METHOD DETAILS

Western blot

Larvae (25 per sample) were lysed in RIPA buffer supplemented with protease and phosphatase inhibitors. Supernatants were run on SDS-PAGE gels and transferred to PVDF membranes. Disc1 protein was detected using Abcam ab191455. This antibody is directed to an internal region of human Disc1 that has 100% conservation with zebrafish residues 511–527.

Embryo and larval behavioral phenotyping

In the photomotor response assay, automated multiplex sensorimotor response assay, and strobe light assay, we used cousins (embryos from WT x WT crosses versus KO x KO crosses; of which the WTs and KOs breeders were derived from a Het x Het cross). Our rationale was that cousins are genetically similar and, importantly, are practical controls to use for high-throughput behavioral screens. It would be challenging to genotype and conduct high-throughput chemical screens on WT and KO larvae derived from Het x Het crosses. This is relevant because one of the goals of the present study was to identify behavioral endpoints in larval *disc1* zebrafish that may be leveraged in high-throughput chemical screens in future studies aimed at identifying novel small molecules to ameliorate schizophrenia-related phenotypes. Importantly, to confirm the phenotypes identified in Figures 2 and 4 did not result from background mutations in our colony, we examined the sensorimotor responses of *disc1* mutants derived from Het incrosses and found similar results (Figure S6).

Photomotor response

Fertilized eggs were obtained from 10-min timed matings. For this assay 28 hpf were used. Embryos (10 per well), stage-matched using morphological developmental landmarks and somite number,[79] were loaded into flat-bottom 96-well plates (black wells with clear bottom). The plated embryos were dark-adapted inside the behavioral apparatus. The stimulus in this assay is two 1 s pulses of high-intensity visual wavelength light (300–700 nm, 52 μW/mm^2, 38,000 lux) delivered at t = 10 and 20 s. This assay was performed using on the Zebrabox (ViewPoint, Lyon, France) in a room at 28°C temperature.

Somite counting

Somite production in zebrafish is linked to their overall developmental progression and has been used to accurately determine embryonic age given they are produced every 30 min between 10.5 and 24 hpf.[80] Images were captured using diffractive oblique microscopy and somites were counted by 2 independent blinded observers.

F-actin staining

Embryos (28 hpf) were fixed in 4% paraformaldehyde overnight, permeabilized with 2% Triton X-100 and stained with Alexa Fluor 594 Phalloidin (Invitrogen) in phosphate buffered saline with 1% bovine serum albumin. Embryos were mounted in low melt agarose and z stack images were captured on a Keyence BZ-X710 Microscope.

Automated multiplex sensorimotor response assay

For this assay, 3 light stimuli (red light: 650 nm, 11 $\mu W/mm^2$, blue light: 560 nm, 18 $\mu W/mm^2$, and violet light: 400 nm, 11 $\mu W/mm^2$) and 2 acoustic stimuli (60 dB low-intensity and 70 dB high-intensity) were used. There were 10 assays: 2 acoustic stimulus response assays, 5 visual stimulus response assays, and 3 combined acoustic and visual stimulus response assays. The temporal series of assays was assembled to maximize the capture of sensorimotor behavioral responses.[25] At 7 dpf, larvae (8 per well) were loaded into wells of clear flat-bottom 96-square-well plates filled with E3 medium (300 μL). After an acclimation period in the enclosed platform in the dark, the 10 serial behavioral assays were conducted over 7 min and locomotor activity was captured by video using an infrared camera.

Whole-brain activity and morphology

Fertilized eggs were obtained from 10-min timed matings. Per established protocols to obtain sufficient numbers of mutant animals and sibling controls for analysis, a homozygous female was mated with a heterozygous male[51]; there was no differences between *disc1* wildtypes and heterozygotes. At 7 dpf, larvae (10 per well) were loaded into clear flat-bottom 96-square-well plates. After an acclimation period in the enclosed behavioral platform (in the dark), a single high magnitude acoustic stimulus (70 dB) was delivered using push-style solenoids to tap the stage. This was conducted in the same behavioral platform used for the automated multiplex sensorimotor response assay described above.[25] Following the stimulus, a 2-min incubation was performed to allow maximal phosphorylation of neuronal ERK.[49] Subsequently, the plate was removed from the behavioral platform and larvae were rapidly fixed in 4% paraformaldehyde in phosphate buffered saline with 0.25% Triton X-100 overnight. To ensure rapid fixation, i.e. less than 10 s after removal from the platform, larvae were poured into a mesh sieve and immediately submerged in fixative. Following fixation, the pigment on larvae was bleached with a 1% H_2O_2/3% KOH solution. The antibodies used for immunofluorescent staining were anti-phosphorylated-ERK (Cell Signaling CAT#4370), anti-total-ERK (Cell Signaling CAT#4696), and Alexa-fluorophore conjugated secondary antibodies (Life Technologies); all antibodies were diluted 1:500. Images were captured using a Zeiss LSM 880 confocal microscopes with a 20×/1.0 NA water-dipping objective. Following imaging, single larvae were genotyped.

Strobe light response assay

At 7 dpf, larvae (10 per well) were loaded into 96-well plates and placed inside the Zebrabox (ViewPoint, Lyon, France) which was located in a room at 28°C. After an acclimation period in the dark, alternating 1-min intervals of darkness and 10 Hz strobe light were delivered during the 7-min assay. The strobe light was set at 10 Hz [white light alternated between 100 ms at the 100% setting, (7.8 $\mu W/mm^2$), and 100 ms at 0%]. An infrared camera recorded locomotor activity in each well.

Behavioral testing room and adult fish handling

Animals were obtained from heterozygous incrosses; WTs are sibling WTs. Care was taken to size and age match animals (1-year old). Males and females were separated prior to the assay day. All fish were not feed prior to the assay to avoid the effects of satiety. Testing occurred between 9a.m. and 5 p.m. Fish were transported from the animal room to the procedure room and given 1 h prior to the start of the assay to acclimate. The behavioral testing room was 28°C. All behavioral assay tanks were sandpapered to reduce reflection and blocked with thick white paper. Assays were performed by alternating WT and mutant fish. Digital videos were captured using a Point Gray Flea3 camera and analyzed using Actual-Track Video Tracking Software (Actual Analytics, Edinburgh, UK). Detection features were set to track the center of the fish.

Novel tank diving test

The behavioral arena was 27 × 6 × 15 cm (L x W x H) with 3 sides sandpapered and covered in white paper, and one side left clear (the viewing side). The water level was 9 cm. One zebrafish was gently netted and placed in the tank. Video was captured for 15 min. To analyze the videos, the area of the arena containing water was divided into horizontal zones. The parameters analyzed were total time, distance traveled, and

average time spent per visit to each zone (top and bottom of the tank). In addition, latency to first entry into the top zone, number of transitions into the top zone, and mean speed was measured.

Light-dark preference test

The behavioral arena was 21 × 10 × 11 cm (L x W x H) with water filled to a height of 9 cm. Half of the tank was blocked with white paper and the other half with black paper. The top of the tank was left open and was the viewing side. An adult fish was gently netted and placed in the dark zone of the tank and recorded for 6 min. The parameters measured were total time in the light zone, latency to first entry into the light zone, number of transitions into the light zone, and average time per visit to the light zone.

Three chamber shoaling preference test

The arena was 32 × 23 × 18 cm (L x W x H) with water filled to a height of 14 cm. It was segmented into 3 separate compartments: the no stimulus compartment, the testing compartment, and the social stimulus compartment. Three sides of the tank were sandpapered and covered in white paper. One side was left open and was the viewing side. Five fish were placed into the stimulus compartment of the arena and given 30 min to acclimate. The stimulus fish were a mix of male and female conspecifics. The test subject was gently netted and placed into the testing compartment. Digital videos were captured for 10 min. To analyze the videos, the chamber where the zebrafish was located in was divided into 4 parts: the social zone (25%), middle (50%) and asocial zone (25%). The parameters measured were total time in the social zone, total time in the asocial zone, average time per visit to the social zone, and average time per visit to the asocial zone.

Shoal cohesion

The arena was 27 × 6 × 15 cm (L x W x H) with water filled to a height of 11.5 cm. Three sides were sandpapered and covered in white. One side was left clear and was used as the viewing side. Six fish were gently netted and placed into a small opaque holding tank for 10 min. The fish were gently poured into the behavioral arena. The fish were given 3 min to acclimate. Digital videos were captured for 3 min. The average pairwise fish-to-fish distance was determined by tracking the 15 pair interactions every 0.3 s for 3 min. The average nearest neighbor and the furthest neighbor was also measured.

QUANTIFICATION AND STATISTICAL ANALYSIS

PMR: Videos were captured and movement was registered as motion indexes that were calculated by frame differencing serial images of each well over the 30 s assay.[23] Automated multiplex sensorimotor response assay: The motion index for each well was calculated by frame differencing.[25] Whole-brain activity and morphology. To generate a whole-brain activity map we used a nonlinear volume registration algorithm.[49] Next, multiple brains were registered into the Z-brain atlas and statistical differences between the groups (mutant and sibling controls) were calculated using Mann-Whitney U statistic *Z* score for each voxel with an FDR ≤ 0.05.[49] Strobe light response assay: The threat response behavior was quantified by measuring the overall motion in each well.[24] Statistical analysis: Statistical analysis was performed using a Student's t-test (two-tailed, unpaired, unequal variance). To adjust for multiple hypothesis testing a two-stage step-up method (Benjamini, Krieger, and Yekutieli) for false discovery rate (FDR) adjustment with a threshold for statistical significance of $q < 0.05$. Error bars in line graphs represent standard deviation unless otherwise noted. In box and whisker plot, the box in the plot represents the 25th percentile to the 75th percentile, the line across the box represents the median, and the whiskers are the maximum and minimum data-point values. Adult behavioral assays: Digital videos were captured using a Point Gray Flea3 camera and analyzed using Actual-Track Video Tracking Software (Actual Analytics, Edinburgh, UK). Detection features were set to track the center of the fish.